PGR5 is needed for redox-dependent regulation of ATP synthase both in chloroplasts and in cyanobacteria

Lauri Nikkanen[1]*, Laura T. Wey[1], Russell Woodford[2], Henna Mustila[1], Maria Ermakova[2], Eevi Rintamäki[1], and Yagut Allahverdiyeva[1]*

[1]Molecular Plant Biology, Department of Life Technologies, University of Turku, Finland

[2]School of Biological Sciences, Monash University, Australia

*Co-corresponding authors

Correspondence:

Lauri Nikkanen, Molecular Plant Biology, Department of Life Technologies, University of Turku, Turku 11 FI- 20014, Finland. E-mail: lenikk@utu.fi

Yagut Allahverdiyeva, Molecular Plant Biology, Department of Life Technologies, University of Turku, Turku 11 FI-20014, Finland. E-mail: allahve@utu.fi

SUMMARY

- Control of the proton motive force (*pmf*) via regulation of ATP synthase constitutes a key mechanism for photosynthetic organisms to maintain redox balance and induce photoprotective mechanisms under light fluctuations.
- Using time-resolved electrochromic shift measurements in various photosynthetic organisms, we found that ATP synthase is dynamically regulated during light fluctuations. While light-induced reduction of the $CF_1\gamma$ subunit is known to activate chloroplast ATP synthase, it did not account for the regulation in fluctuating light in *Arabidopsis thaliana*, suggesting alternative mechanisms.
- The PROTON GRADIENT REGULATION 5 (PGR5) protein is important for photoprotection in algal and plant chloroplasts. PGR5 has been proposed to facilitate cyclic electron transport around PSI (CET), but it also affects ATP synthase activity. The physiological role of cyanobacterial Pgr5 has remained elusive.
- We characterised a Δ*pgr5* mutant of *Synechocystis* sp. PCC 6803 and investigated *pmf* dynamics in *pgr5* mutants of *Chlamydomonas reinhardtii*, *Arabidopsis*, and the C_4 grass *Setaria viridis*. While PGR5 was not required for CET in *Synechocystis*, it was needed for downregulating ATP synthase under high irradiance in all tested organisms via a thiol redox state dependent mechanism.
- As AtPGR5 interacted with $AtCF_1\gamma$, PGR5 may have a conserved function as an inhibitor of ATP synthase.

KEYWORDS: Photosynthesis, ATP synthase, proton motive force, chloroplast, cyanobacteria, Arabidopsis, electrochromic shift

INTRODUCTION

Oxygenic photosynthesis by plants, algae, and cyanobacteria uses light energy to drive oxidation of water to produce ATP and NADPH for CO_2 fixation and other cellular processes. In their natural habitats, oxygenic photosynthetic organisms undergo constant fluctuation of irradiance. Mechanisms to adjust the redox homeostasis in chloroplasts and cyanobacterial cells have evolved to prevent energy-consuming futile reactions and damage to the photosynthetic machinery and other biomolecules via generation of reactive oxygen species (ROS) by the photosynthetic apparatus. ROS can be generated as a result of excitation imbalance between the photosystems, or when electron transport rate exceeds the sink capacity of the reactions downstream of the photosynthetic electron transport chain (PETC). Resulting accumulation of reduced electron carriers in the PETC triggers charge recombination reactions within the photosystems and direct reduction of O_2, generating highly reactive ROS such as superoxide ($O_2^{\bullet-}$) and hydrogen peroxide (H_2O_2) at PSI and singlet oxygen ($^1O_2$) primarily at PSII (Foyer & Hanke, 2022). PSI and its iron sulphur clusters are particularly vulnerable to over-reduction-induced damage, and plants, algae, and cyanobacteria invest heavily in their protection (Tiwari et al., 2016, 2024). These protective mechanisms involve cyclic electron transport around PSI (CET), redistribution of excitation energy between the photosystems via state transitions, non-photochemical quenching (NPQ), and inhibition of PQH_2 oxidation at the cytochrome b_6f complex, known as photosynthetic control (Degen & Johnson, 2024; Eckardt et al., 2024; Nikkanen et al., 2021; Shimakawa et al., 2016; Tikkanen & Aro, 2014). Additionally, in photosynthetic organisms apart from angiosperms, flavodiiron proteins provide a photoprotective electron sink on the acceptor side of PSI by catalysing controlled reduction of O_2 to water (the Mehler-like reaction) (Allahverdiyeva et al., 2013; Ilik et al., 2017).

As photosynthetic control and NPQ (in plants and algae) are induced by acidic pH of the thylakoid lumen, an important mechanism to maintain photosynthetic redox balance involves control of the proton motive force *(pmf)* via regulation of the thylakoid ATP synthase (Kanazawa et al., 2017; Takagi et al., 2017). The pH-dependent component of *pmf* (ΔpH), is generated by translocation of protons from the stroma (or the cytosol in cyanobacteria) to the lumenal side of the thylakoid membrane by linear and cyclic electron transport as well as consumption of protons on the stromal side. The proton gradient is released mainly via efflux through the ATP synthase, providing the driving force for ATP synthesis. Proton-conductivity of the ATP synthase is therefore an important regulatory factor for adjusting the magnitude of the *pmf*.

In addition to ΔpH, the *pmf* comprises an electric field component ($\Delta\Psi$). $\Delta\Psi$ derives from charge separation within the photosystems, the positive charge of protons, and pumping of cations (e.g. K^+, Ca^{2+} and Mg^{2+}) in and anions (e.g. Cl^-) out of the lumen by ion transporters in the thylakoid membrane (Armbruster et al., 2017). ΔpH and $\Delta\psi$ are thermodynamically equivalent and both drive

ATP synthesis (Hangarter & Good, 1982). However, build-up of sufficient ΔpH over the thylakoid membrane is required for induction of photoprotective mechanisms upon sudden increases in light intensity, namely dissipation of excessive excitation energy as heat in NPQ (Krishnan-Schmieden et al., 2021; Niyogi & Truong, 2013) and photosynthetic control (Degen & Johnson, 2024; Tikhonov et al., 1981). These mechanisms prevent over-reduction of the electron transport chain and photodamage to PSI. Conversely, it is also important to down-regulate ΔpH (and consequently, NPQ and photosynthetic control) upon sudden decreases in irradiance in order to maintain sufficient supply of electrons on the acceptor side of the electron transfer chain for carbon fixation in the Calvin–Benson cycle (CBC).

ATP synthase is regulated via several mechanisms. The $F_1\varepsilon$ (epsilon) subunits of the chloroplast (CF_0CF_1) ATP synthase (Feniouk et al., 2006) and the cyanobacterial ATP synthase (Imashimizu et al., 2011; Murakami et al., 2018) have inhibitory roles preventing ATP hydrolysis. $F_1\varepsilon$ undergoes conformational changes triggered by *pmf* generation and changes in ATP/ADP ratio, allowing inhibition of ATP hydrolysis (Feniouk et al., 2006; Richter & McCarty, 1987). Moreover, upon dark-to-light transitions, the chloroplast ATP synthase is activated by thioredoxin (TRX)-mediated reduction of a disulphide in the γ subunit ($CF_1\gamma$) (Akiyama et al., 2023; McKinney et al., 1978; Nalin & McCarty, 1984). $CF_1\gamma$ is kept in an inactive oxidised state in darkness to avoid hydrolysis of ATP by reverse activity or loss of the proton gradient (Hahn et al., 2018; Hisabori et al., 2013; Kohzuma et al., 2017). Maintenance of adequate dark-*pmf* via ATP synthase dark-light regulation is also needed for powering the insertion of new proteins into the thylakoid membrane via the Tat- and Sec-pathways to maintain the integrity of the photosynthetic apparatus (Kohzuma et al., 2017). $CF_1\gamma$ is reduced in seconds upon illumination, which lowers the threshold *pmf* for activation of the ATP synthase (Buchert et al., 2021; Kohzuma et al., 2017; Konno et al., 2012; Kramer et al., 1990; Nikkanen et al., 2018). In turn, as ΔpH also facilitates reduction of the $CF_1\gamma$ disulphide bond (Sekiguchi et al., 2024), while dissipation of ΔpH promotes oxidation of $CF_1\gamma$ (Sekiguchi et al., 2022). F- and m-type chloroplast TRX isoforms have been understood to be mainly responsible for light-dependent reduction of $CF_1\gamma$ (Schwarz et al., 1997; Sekiguchi et al., 2020), and chloroplast TRX-like proteins catalyse the oxidation of the subunit in the dark (Sekiguchi et al., 2022). Additionally, *in vivo* studies have revealed the involvement of the NADPH-dependent TRX system (NTRC) in $CF_1\gamma$ reduction in low light conditions (Carrillo et al., 2016; Nikkanen et al., 2016), while the atypical TRX CDSP32 was recently suggested to play a role in reduction of $CF_1\gamma$ in potato (Rey et al., 2024).

Reduction of $CF_1\gamma$ constitutes an on/off switch controlling the activation of the ATP synthase upon the onset of illumination in chloroplasts of plants and algae, and does not occur in mitochondria or in cyanobacteria (Hisabori et al., 2013). The cyanobacterial γ subunit still has a role in preventing ATP hydrolysis however, via an ADP-dependent mechanism (Sunamura et al., 2010). Moreover, the small

134 AtpΘ protein (Song et al., 2022) has been reported to function as an inhibitor of the cyanobacterial
135 ATP synthase in the dark and in low *pmf* conditions, preventing ATP hydrolysis and collapse of the
136 proton gradient. Interestingly, the $F_1\alpha$ (AtpA) and $F_1\beta$ (AtpB) subunits of the ATP synthase also
137 contain conserved Cys residues, and $F_1\alpha$ has been identified as a prospective TRX target in
138 cyanobacteria (Guo et al., 2014; Lindahl & Florencio, 2003), and $F_1\beta$ in plants (Balmer et al., 2006).
139 Moreover, the mitochondrial ATP synthase in *Xenopus laeviis* oocytes is regulated by reversible
140 oxidation of thiols in the $F_1\alpha$ subunit (Cobley et al., 2020).

141 There are also other regulatory mechanisms that adjust the activation state of the ATP synthase
142 according to the metabolic state of the stroma or cytosol, such as substrate (ADP and P_i) availability
143 (Avenson et al., 2005; Kanazawa & Kramer, 2002; Takagi et al., 2017). High CO_2 supply results in
144 increase of chloroplast ATP synthase activity by a mechanism that is independent of $CF_1\gamma$ redox state
145 (Kiirats et al., 2009; Kohzuma et al., 2013). Another potential regulatory mechanism involves
146 phosphorylation of the β subunit (del Riego et al., 2006).

147 Additionally, thylakoid conductivity and the *pmf* can be adjusted through the activities of ion channels
148 and transporters in the thylakoid membrane (Spetea et al., 2017). A lack of the K^+/H^+ exchanger
149 KEA3, the two-pore K^+ channel TPK3, or the Cl^- channels CLCe and VCCN1 has been shown to
150 affect the *pmf* and/or induction and relaxation of NPQ in plants (Armbruster et al., 2014; Carraretto
151 et al., 2013; Herdean, Nziengui, et al., 2016; Herdean, Teardo, et al., 2016; von Bismarck et al., 2023;
152 Wang & Shikanai, 2019). Similarly, lack of the cyanobacterial K^+ channel SynK resulted in decreased
153 ΔpH generation and impairment of photosynthetic control in the model cyanobacterium *Synechocystis*
154 sp. PCC 6803 (*Synechocystis*) (Checchetto et al., 2012). Controlling the ionic environment of the
155 thylakoid membrane is particularly important to avoid drastic increases in ΔΨ, which result in
156 production of damaging $^1O_2$ via recombination reactions in PSII (Davis et al., 2016).

157 Plants deficient in the PROTON GRADIENT REGULATION 5 (PGR5) protein suffer from impaired
158 *pmf* generation (Munekage et al., 2002). In plant chloroplasts, PGR5 forms redox-dependent
159 heterodimers with PGRL1 (PGR5-LIKE 1), which have been proposed to mediate or regulate cyclic
160 electron transport (CET) from ferredoxin to the plastoquinone pool (DalCorso et al., 2008; Hertle et
161 al., 2013; Yamamoto & Shikanai, 2019), contributing to *pmf* formation (Wang et al., 2015). More
162 recently, a functional PGRL1-analogue was identified also in cyanobacteria (Dann & Leister, 2019).

163 The *pgr5* knockout plants are unable to induce photosynthetic control and NPQ during transitions
164 from low to high light (HL) (Munekage et al., 2002; Suorsa et al., 2012; Yamamoto & Shikanai,
165 2019). Consequently, exposure of *pgr5* mutant plants to HL results in over-reduction of the electron
166 transport chain and photodamage to the iron sulphur clusters of PSI (Tiwari et al., 2016, 2024).
167 Accordingly, the lack of PGR5 is lethal in fluctuating light conditions in *Arabidopsis thaliana*

168 *(Arabidopsis)* (Suorsa et al., 2012; Tikkanen et al., 2010) and severely inhibits growth of the model C_4
169 plant *Setaria viridis* (Woodford et al., 2024) as well as of the model green alga *Chlamydomonas*
170 *reinhardtii (Chlamydomonas)* (Jokel et al., 2018). *Synechocystis* cells deficient in a PGR5-orthologue
171 (SynPgr5) suffer from slightly increased HL-sensitivity (Yeremenko et al., 2005), but no growth
172 impairment was observed in fluctuating light conditions (Allahverdiyeva et al., 2013). Interestingly,
173 however, there is strong selection pressure against overexpression of SynPgr5 (Margulis et al., 2020).

174 The physiological functions of PGR5 and PGRL1 remain controversial, with some reports linking the
175 proteins to regulation of linear instead of cyclic electron transport from PSI (Johnson et al., 2014;
176 Joliot & Johnson, 2011; Maekawa et al., 2024; Nandha et al., 2007; Rantala et al., 2020; Takagi &
177 Miyake, 2018; Tikkanen et al., 2015), or regulation of the Q-cycle at the cytochrome b_6f complex
178 (Buchert et al., 2020). Impaired *pmf* generation and induction of photoprotection in the *pgr5* mutant
179 could also derive from the inability of the mutant plants to limit the conductivity of the thylakoid
180 membrane under HL (Avenson et al., 2005; Degen et al., 2023; Nikkanen et al., 2018). Interestingly,
181 elevated thylakoid (ATP synthase) conductivity upon HL exposure was not observed in isolated and
182 ruptured *pgr5* mutant chloroplasts (Wang et al., 2018). This suggests that a stromal component that is
183 lost in ruptured chloroplasts plays a role in the effect of PGR5 on thylakoid conductivity.

184 In the current study, we elucidated the dynamics of *pmf* regulation under light in a variety of
185 photosynthetic organisms focusing on the potential role of PGR5. We performed *in vivo*
186 characterisation of photosynthetic electron transport and *pmf* formation in *Synechocystis,*
187 *Chlamydonomas*, *Arabidopsis,* and *S. viridis.* Our results reveal that in *Arabidopsis*, dynamic
188 regulation of ATP synthase conductivity during fluctuations in light intensity is independent of the
189 thiol redox state of the $CF_1\gamma$ subunit. We show that downregulation of the ATP synthase activity upon
190 transitions to HL depends on PGR5 as well as the thiol redox state of the stroma or cytosol in both
191 chloroplasts and cyanobacteria. PGR5 is only essential for oxidation of the PETC in plants though,
192 and not in cyanobacteria. Moreover, we demonstrate that cyanobacterial SynPgr5 is not needed for
193 CET, and suggest that the observed effect of plant PGR5 on cyclic electron transport may be an
194 indirect consequence of misregulation of ATP synthase and increased photoinhibition of PSI.

195

196 **RESULTS**

197 **Dynamic changes in thylakoid conductivity are independent of the thiol redox state of $CF_1\gamma$ in**
198 **plants**

199 In plants and algae, measurement of dark-interval relaxation kinetics (DIRK) of the electrochromic
200 shift (ECS) signal has been widely used for *in vivo* determination of the magnitude of the *pmf*,

201 partitioning of the *pmf* between ΔpH and ΔΨ, as well as the conductivity of the thylakoid membrane,
202 which is mainly determined by the activity of ATP synthase (Bailleul et al., 2010; Cruz et al., 2001,
203 2005; Sacksteder & Kramer, 2000; Schreiber & Klughammer, 2008). Recently, a reliable method to
204 measure ECS has also been developed for cyanobacteria (Nikkanen et al., 2020; Santana-Sánchez et
205 al., 2023; Viola et al., 2019).

206 Time-resolved ECS analysis in wild type (WT) *Arabidopsis* revealed that upon the onset of
207 illumination of dark-adapted leaves, the conductivity of the ATP synthase (g_H+) initially decreased for
208 c.a. 30 s (Fig. 1a), as observed previously (Guinea Diaz et al., 2020; Nikkanen et al., 2018). This
209 initial decrease in g_H+ allowed transient build-up of *pmf* (Fig. 1b) and induction of photoprotective
210 mechanisms (Fig. 1c–d) in order to avoid over-reduction of the electron transport chain when redox-
211 regulated CBC enzymes such as Fructose-1,6-bisphosphatase (FBPase) are not yet activated (i.e.
212 reduced). After the initial decrease, at c.a. 30 s of illumination, g_H+ started to increase gradually,
213 resulting in decrease of *pmf* to a steady-state level (Fig. 1a–b). Importantly, these changes in g_H+ did
214 not correlate with the thiol redox state of $CF_1\gamma$. $CF_1\gamma$ was rapidly reduced at the onset of illumination,
215 becoming almost fully reduced after 20 s, and remained reduced thereafter (Fig. 1e). In contrast,
216 FBPase remained mostly oxidised (inactive) for a full minute in low light, and only became partially
217 reduced when leaves were exposed to HL (Fig. 1f). These results demonstrate that the initial
218 downregulation of ATP synthase activity during dark-to-light transitions is independent of $CF_1\gamma$ redox
219 state and must occur via another mechanism.

220 When WT *Arabidopsis* leaves were exposed to a light regime where light intensity alternates between
221 periods of low light (LL) and HL, mimicking natural fluctuations, intricate regulatory dynamics of the
222 *pmf* and g_H+ could be observed. During LL phases, g_H+ increased substantially, which contributed to
223 a rapid decline in *pmf* (Fig. 1a–b). This upregulation of g_H+ allowed relaxation of photosynthetic
224 control (measured as donor-side limitation of PSI) and NPQ (Fig. 1c–d), allowing sufficient supply of
225 electrons to stromal reactions. Similarly to downregulation of g_H+ during dark-to-light transitions, the
226 upregulation of g_H+ during LL happened independently of the thiol redox state of $CF_1\gamma$, which
227 remained fully reduced throughout the change in light intensity (Fig. 1e).

228 In contrast to LL phases, g_H+ was rapidly downregulated in WT leaves during HL phases (Fig. 1a),
229 enabling sufficient *pmf* build-up (Fig. 1b) for induction of photosynthetic control and NPQ (Fig. 1c–
230 d). Again, the decrease in g_H+ did not coincide with oxidation of $CF_1\gamma$, which remained fully reduced
231 (Fig. 1e).

232

233 **Thylakoid conductivity is dynamically regulated under fluctuating light also in cyanobacteria**
234 **and unicellular algae**

When WT *Synechocystis* cells were subjected to sudden fluctuations between moderate light (ML) and HL, time-resolved ECS-DIRK measurements revealed downregulation of g_{H^+} during HL phases (Fig. 2a), resembling that observed in *Arabidopsis*. As in plants, this downregulation likely occurs to maintain an adequate *pmf* (Fig. 2b) for induction of photosynthetic control. Accordingly, strong donor side limitation of PSI (Y(ND)) was measured during HL phases (Fig. 2d) indicative of limitation of electron transport from Cyt b_6f. In contrast to *Arabidopsis*, g_{H^+} remained low during the ML phases of the experiment (Fig. 2a).

We also probed the *pmf* and g_{H^+} dynamics under fluctuating light in the unicellular green alga *Chlamydomonas*. While *pmf* underwent similar changes as in plants and in cyanobacteria (Fig. 3a), no clear downregulation of g_{H^+} was observed during HL, and during the LL phases g_{H^+} remained low (Fig. 3b).

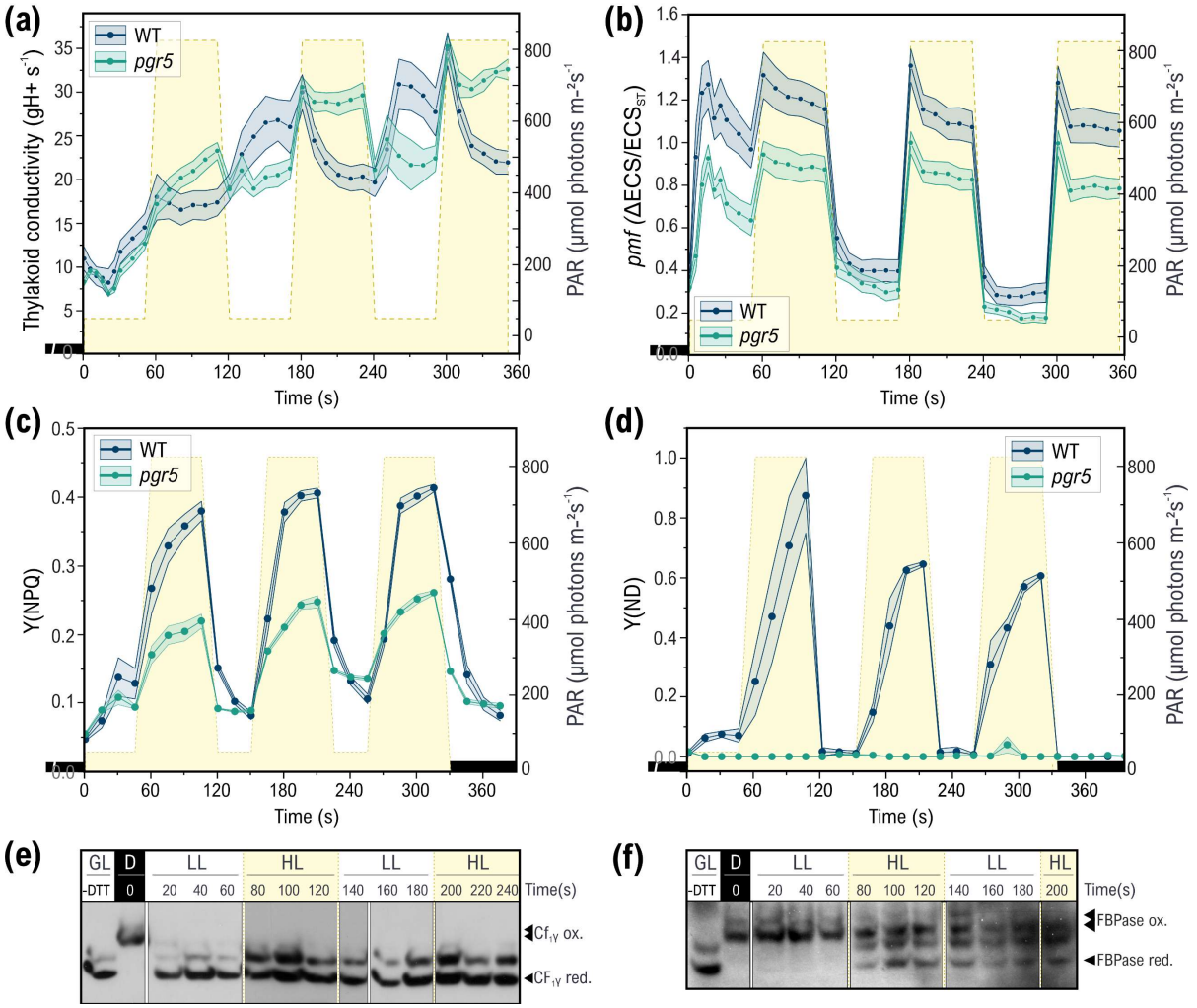

Figure 1. Effect of PGR5 and $CF_1\gamma$ redox state on *pmf,* thylakoid conductivity, and photoprotection in fluctuating light in *Arabidopsis*. (a) Proton conductivity of the thylakoid membrane (g_{H^+} s^{-1}) and **(b)** magnitude of the *pmf* in fluctuating light, as determined from dark-interval relaxation kinetics (DIRK) of the ECS signal. ECS was measured from dark-adapted WT-gl1 and *pgr5* mutant *Arabidopsis* leaves under a light regime alternating between 1 min periods of low (50

251 µmol photons $m^{-2}s^{-1}$) and high light (825 µmol photons $m^{-2}s^{-1}$). The values in (a) are averages from 9 and in (b) 11 biological
252 replicates ± SEM. **(c)** Quantum yield of non-photochemical quenching (Y(NPQ)) and **(d)** fraction of oxidised P700 (donor
253 side limitation of PSI, Y(ND)) in a fluctuating light regime supplemented with saturating pulses at 15 s intervals. The values
254 in C–D are averages from 3 biological replicates ± SEM. **(e)** A mobility shift assay of the in vivo thiol redox state of the
255 $CF_1\gamma$ subunit of the chloroplast ATP synthase and **(f)** the CBC enzyme FBPase in fluctuating light (1 min periods of 50
256 µmol photons $m^{-2}s^{-1}$, LL, and 825 µmol photons $m^{-2}s^{-1}$, HL, in WT leaves. The break between the 140 and 160 sec samples
257 in (e) represents division between two gels.

258

259 **PGR5 is needed for downregulation of thylakoid conductivity under strong illumination across**
260 **photosynthetic organisms**

261 During dark-to-LL transitions, the *Arabidopsis pgr5* mutant plants had a lower *pmf* than WT (Fig.
262 1B), as shown previously and attributed to lower linear electron transport rates (Nikkanen et al.,
263 2018). In fluctuating light, the *pgr5* mutants were unable to decrease g_H+ during HL phases (Fig. 1a),
264 resulting in partial loss of *pmf* (Fig. 1b), in agreement with previous studies (Avenson et al., 2005;
265 Nikkanen et al., 2018). The mutant plants also exhibited impaired induction of NPQ (Fig. 1c) and
266 photosynthetic control, resulting in an inability to oxidise P700 (Fig. 1d). Interestingly, and in contrast
267 to their behaviour during HL phases, *pgr5* mutant plants showed a lower g_H+ and slightly lower *pmf*
268 than WT during LL phases (Fig. 1a–b).

269 The *Arabidopsis pgr5-1* mutant used in our experiment has been reported to also contain an additional
270 mutation in the At2g1724 gene, which slightly exacerbates PSI photoinhibition in the mutant (Wada
271 et al., 2021). Mutants where an intact At2g1724 has been re-introduced (*pgr5*^{hope1} and *pgr5-Cas*) are,
272 however, also unable to induce photosynthetic control to oxidise PSI (Wada et al., 2021), and have
273 similarly elevated g_H+ and diminished *pmf* as the *pgr5-1* mutant (Maekawa et al., 2024; Penzler et al.,
274 2022). While it is therefore unlikely that the At2g1724 mutation in *pgr5-1* plants would have a
275 significant effect on the phenotypes examined in the current study, we confirmed this by repeating the
276 ECS experiment (Fig. 1a–b) also with the *pgr5-Cas* mutant (Penzler et al., 2022). Results with *pgr5-*
277 *Cas* plants were similar to the ones with *pgr5-1,* apart from the decrease in *pmf* during initial dark-to-
278 LL transitions being less prominent in *pgr5-Cas* plants than in *pgr5-1* in comparison to WT (Fig. S1).
279 Moreover, while a diminished proton flux (v_H+) in LL and immediately upon shifts to HL was
280 measured in *pgr5-1* mutants in comparison to WT (Fig. S2a), this decrease was absent in *pgr5-Cas*
281 plants, which instead exhibited elevated v_H+ during the first HL phase (Fig. S1c).

282 We proceeded to investigate whether lack of SynPgr5 affects regulation of g_H+ in *Synechocystis*.
283 Elevated g_H+ was indeed detected upon exposure of Δ*pgr5* cells to HL after illumination in moderate
284 light (ML) in a fluctuating light regime (Fig. 2a, c), concomitant with diminished *pmf* (Fig. 2b, c). The
285 increased g_H+ was not due to an elevated amount of ATP synthase, as the protein level of AtpB

286 remained unchanged in the mutant (Fig. S3). Increased thylakoid conductivity resulted in
287 diminishment of *pmf* (Fig. 2b). Despite the elevated g_H+ and in contrast to AtPGR5-deficient
288 *Arabidopsis*, no decrease in donor-side limitation (indicative of impairment of photosynthetic control)
289 or increase in acceptor side limitation of PSI was detected during transitions to HL in *Synechocystis*
290 Δ*pgr5* cells (Fig. 2c–d). Interestingly, a slight, albeit statistically non-significant decrease in donor
291 side limitation of PSI was detected in Δ*pgr5* upon transitions from HL to LL (Fig. 2d). This may be
292 due to faster deactivation of photosynthetic control by faster dissipation of *pmf* (Fig. 2b).

293 The ability of the *Synechocystis* Δ*pgr5* strain to maintain sufficient PSI oxidation for unimpaired
294 photosynthetic activity may be due to the strong electron sink capacity of the Mehler-like reaction
295 catalysed by flavodiiron proteins (FDPs) under light (Allahverdiyeva et al., 2013). Therefore, we
296 tested the PSI oxidation capacity of a Δ*flv3 pgr5* double mutant strain, which is deficient in both
297 SynPgr5 as well as the Flv1/3 hetero-oligomers (Fig. S3) that are mainly responsible for the strong,
298 rapidly induced Mehler-like reaction (Santana-Sanchez et al., 2019). We detected slightly aggravated
299 impairment of PSI oxidation in the double mutant in comparison to the Δ*flv3* mutant during initial LL-
300 to-HL transitions (Fig. 2c) due to slightly increased acceptor side limitation of PSI (Fig. 2d). The
301 additional effect of Pgr5 deficiency was minor compared to lack of Flv3, and no additional
302 aggravation of ferredoxin redox kinetics, CO_2 fixation, or O_2 evolution was observed in Δ*flv3 pgr5* in
303 comparison to Δ*flv3* (Fig. S4). These results indicate that SynPgr5 may affect PSI oxidation also in
304 cyanobacteria, but its importance is minor compared to plants, while flavodiiron proteins have a
305 crucial role. This was also reflected in the growth phenotypes of the strains. In agreement with
306 previous results (Allahverdiyeva et al., 2013), no difference in growth was detected between WT and
307 Δ*pgr5* under fluctuating light, while additional deficiency of Flv3 in Δ*pgr5 flv3* prevented growth
308 entirely (Fig. 2f), similarly to Δ*flv3* (Allahverdiyeva et al., 2013).

309 The Δ*flv3* mutant showed a decreased g_H+ in the HL phases of fluctuating light (Fig. 2a), which
310 allowed it to compensate for diminished v_H+ (Fig. S2b) and maintain WT-level *pmf* (Fig. 2b). The
311 Δ*pgr5 flv3* double mutant, however, exhibited WT-like g_H+, v_H+, and *pmf* (Fig. 2b, Fig. S2b),
312 indicating that the downregulation of g_H+ observed in Δ*flv3* is also at least partly dependent on
313 SynPgr5.

314 To clarify whether SynPgr5 is involved in CET in *Synechocystis* as previously concluded (Dann &
315 Leister, 2019; Yeremenko et al., 2005), we quantified the rates of CET and linear electron transport
316 (LET) in WT and Δ*pgr5* cells using DIRK analysis of near-infrared absorbance difference signals, as
317 described by (Theune et al., 2021). Our results showed that the CET rate was not decreased in the
318 deletion mutant (Fig. 4a), indicating that SynPgr5 is not involved in CET, at least at steady state
319 conditions. It has been previously reported that a *Synechocystis* Δ*pgr5* mutant has a slowed-down rate
320 of P700 oxidation under far-red light as measured (Dann & Leister, 2019), which can be an indication

of decreased CET, although results from such assays should be interpreted with caution (Fan et al., 2007). In contrast to the previous report, we detected no difference between WT and Δ*pgr5* in far-red-induced P700 oxidation rate when measured as the deconvoluted P700 signal using the Dual-KLAS-NIR instrument (Fig. S5).

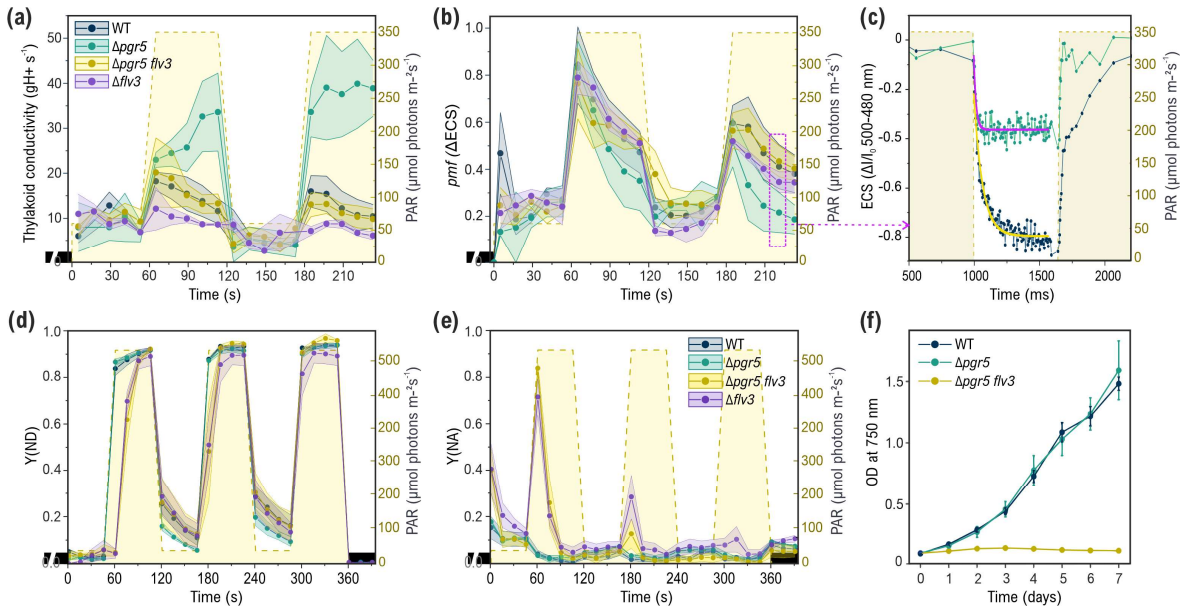

Figure 2. ***Pmf* dynamics, PSI oxidation, and growth under fluctuating light in *Synechocystis*.** Thylakoid conductivity (g_{H^+}) **(a)**, and *pmf* **(b)** were determined by the ECS DIRK method from WT and *Δpgr5* cells. The values in A-B are averages from 3–6 (depending on the quality of the first-order DIRK fit) biological replicates ± SEM. **(c)** Representative ECS decay kinetics in WT and *Δpgr5* cells during the second-to-last 600 ms dark interval in the experiment. First order exponential fits are shown in magenta and yellow. **(d)** Donor (Y(ND)) and **(e)** acceptor side limitation (Y(NA)) of PSI in WT, Δ*pgr5,* Δ*pgr5 flv3*, and Δ*flv3* strains of *Synechocystis* during transitions from low light (25 uE, LL) to high light (525 uE, HL). Y(NA) and Y(ND) were determined from P700 redox kinetics using the saturating pulse method on a DUAL-PAM 100 spectrophotometer. Traces are averages of 3–4 biological replicates ± SEM (ribbons). **(f)** Growth curves (OD 750 nm) of WT, *Δpgr5* and *Δpgr5 flv3* cells under fluctuating light (5 min at 20 µmol photons $m^{-2}s^{-1}$ to 30 sec at 500 µmol photons $m^{-2}s^{-1}$). The values are averages from 3 biological replicates ± SEM.

Near-infrared spectroscopy revealed no significant differences in the deconvoluted redox signals for ferredoxin (Fed), plastocyanin (PC) or P700 between WT and Δ*pgr5* cells upon onset of strong illumination (Fig. 4b). Moreover, analysis of *in vivo* O_2 and CO_2 gas exchange by membrane inlet mass spectrometry (MIMS) showed that oxygen evolution (Fig. 4c), dark respiration rate (Fig. 4d), light-induced O_2 uptake rate indicative of FDP activity (Fig. 4c, e), as well as CO_2 fixation (Fig. 4f) were all unchanged in Δ*pgr5* in comparison to WT cells. When cells were grown under fluctuating light and O_2 gas exchange was measured under similar conditions, however, a slightly elevated light-induced O_2 uptake rate was observed in Δ*pgr5,* although the difference was statistically significant only during the first HL phase (Fig. 5).

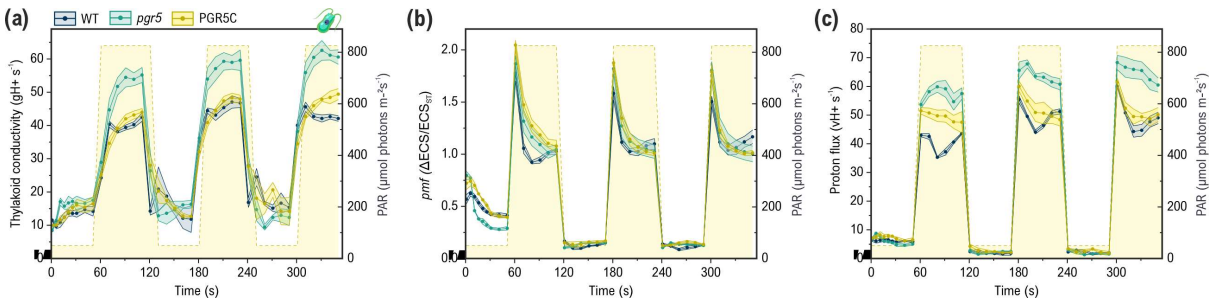

Figure 3. *Pmf* dynamics in *Chlamydomonas reinhardtii* under fluctuating light. (a) Thylakoid conductivity (g_{H^+}). **(b)** *pmf* ($\Delta ECS/ECS_{ST}$). **(c)** Proton flux (v_{H^+}). The ECS signal was measured from WT137c, *pgr5* knockout mutant, and PGR5 complementation line (PGR5C) cells using the same protocol as described in the Figure 1 legend. Values are mean ± SEM from three biological replicates.

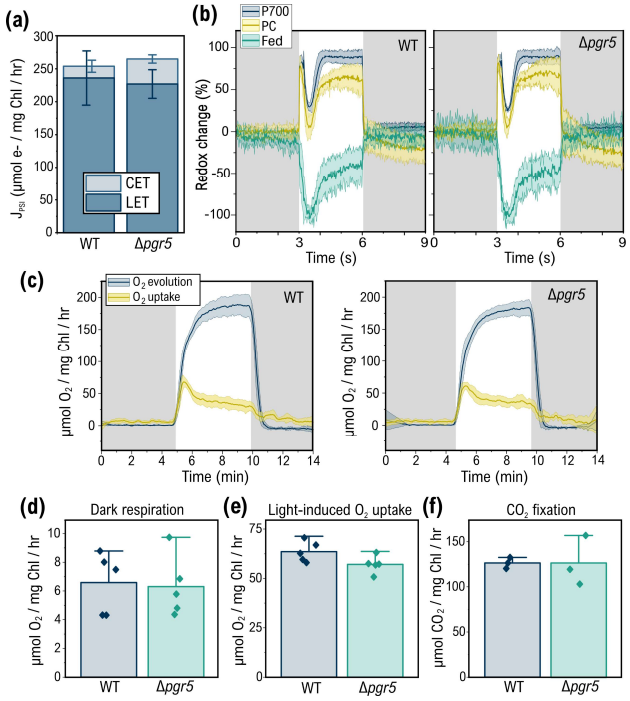

Figure 4. Photosynthetic phenotype of the *Synechocystis Δpgr5* strain. (a) Quantification of LET and CET rates in *Synechocystis* WT and Δ*pgr5*. Chlorophyll was adjusted to 20 µg/ml in BG-11 pH 7.5. Using a Dual KLAS-NIR spectrophotometer, cells were illuminated for 2 min under 500 µmol photons $m^{-2}s^{-1}$ before administering 100x 40 ms dark intervals 10 s apart to monitor the relaxation kinetics of the P700 and PC signals. The measurement was then repeated in the presence of 10µM DCMU to inhibit LET. **(b)** *In vivo* redox kinetics of P700, PC, and Fed in WT and *Δpgr5* strains of *Synechocystis* as monitored with the DUAL-KLAS/NIR spectrophotometer. Dark-adapted cells were illuminated for 3 s with 3000 µmol photons $m^{-2}s^{-1}$. The traces are averages of 7 biological replicates ± SD. **(c)** *In vivo* O_2 gas exchange in WT and Δ*pgr5* cells, as analysed by membrane inlet mass spectrometry (MIMS). Cells were adjusted to 10 µg Chl/ml, and $^{18}O_2$ added in equilibrium with $^{16}O_2$ in order to distinguish O_2 uptake from O_2 evolution. Cells were dark-adapted for 10 min, after which gas exchange was monitored for 5 min in dark, 5 min under 500 µmol photons $m^{-2}s^{-1}$ illumination, and 5 min in post-illumination dark. **(d)** Dark respiration rates as averages of O_2 uptake during the first two minutes of darkness in (e) ± SD. **(e)** Maximum light-induced O_2 uptake rates as averages of O_2 uptake peaks around 30 s of illumination - dark

respiration rate ± SD. **(f)** CO_2 fixation rates as averages of CO_2 uptake rates during the final minute in light in (e) + respiration rate during the first two minutes of darkness.

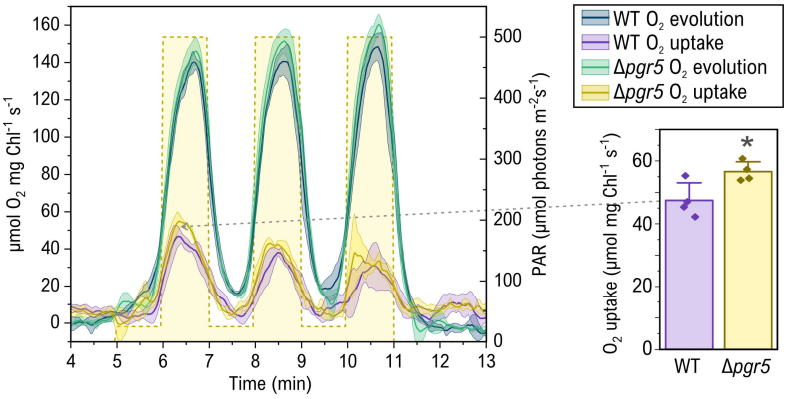

Figure 5. O_2 gas fluxes in fluctuating light in WT and *Δpgr5 Synechocystis* cells. Cells were grown in fluctuating light (1 min 25 µmol photons $m^{-2}s^{-1}$ / 1 min 500 µmol photons $m^{-2}s^{-1}$), and real-time gas fluxes were measured by MIMS mimicking the same light conditions, with a 5 min dark period on either side of 3 LL-HL cycles. The values are averages of 4 biological replicates ± SD. The bar chart shows the maximum O_2 uptake rates + SD during the first HL phase of the experiment (dotted arrow). * indicates statistically significant difference to WT according to a two-sample Student's t-test ($P<0.05$).

There is no PGR5 orthologue identified in the genome of another cyanobacterial model species, *Synechococcus elongatus* sp. PCC 7942 (*Synechococcus*) (Shimakawa et al., 2016). We therefore proceeded to investigate whether the regulation of g_H+ in response to fluctuating light conditions in *Synechococcus* differs from *Synechocystis*. Interestingly, no major difference was observed in comparison to the g_H+ kinetics in *Synechocystis*, with down-regulation of g_H+ occurring during the HL phases after an initial increase (Fig. S6). This suggests that the downregulation of g_H+ in HL is achieved via a different mechanism in *Synechococcus*.

Elevated g_H+ under HL was also observed in the *Chlamydomonas pgr5* mutant, in comparison to WT or a CrPGR5 complementation strain (Fig. 4a). Interestingly, this did not result in lower *pmf* under HL due to elevated proton flux (v_H+) (Fig. 4b, c). Finally, the increase in g_H+ during the HL phases of a fluctuating light regime was also detected in a *pgr5* mutant of the model C_4 grass *S. viridis* (Fig. S7), highlighting a conserved function of PGR5 in regulation of the proton conductivity of ATP synthase from cyanobacteria to chloroplasts in algae, C_3, and C_4 plants.

Elucidating the mechanism of redox-dependent inhibition of thylakoid conductivity

We have previously shown that increasing the reducing capacity of the chloroplast thiol redox regulation systems through overexpression of NTRC in *Arabidopsis* intensifies the downregulation of g_H+ upon increases in light intensity (Nikkanen et al., 2018). We therefore proceeded to investigate

392 potential thiol regulation of thylakoid conductivity or ATP synthase activity, as well as the role of
393 PGR5 in it.

394 Addition of methyl viologen (MV) results in lowered conductivity of the thylakoid membrane, which
395 has been interpreted as prevention of TRX-mediated reduction of the $CF_1\gamma$ disulphide (Kramer &
396 Crofts, 1989). MV facilitates electron transfer from PSI or reduced ferredoxin to O_2 (the Mehler
397 reaction), resulting in generation of ROS (Fujii et al., 1990; Sétif, 2015; Shapiguzov et al., 2019,
398 2020). However, MV is also able to donate electrons to redox-regulated enzymes such as nitrite
399 reductase in spinach (Hirasawa & Tamura, 1980) and glutathione reductase in yeast (Llobell et al.,
400 1986). To further elucidate the relationship between stromal/cytosolic thiol redox state and PGR5-
401 dependent downregulation of thylakoid conductivity, we investigated the effects of MV on
402 chloroplastic thiol-regulated enzymes and *pmf* in *Arabidopsis.* We first determined the *in vivo* thiol
403 Although electron supply to the TRX systems from PSI is limited by MV, addition of MV caused
404 strong reduction of the 2-cysteine peroxiredoxin (2-CysPrx), FBPase, and $CF_1\gamma$ pools even in
405 darkness (Fig. 6a). NTRC, whose redox state is mostly unaffected by light conditions, thereby acting
406 as a buffer system for plastidial redox state (Nikkanen et al., 2018; Zimmer et al., 2021), also became
407 strongly reduced after 90 min of illumination when treated with MV (Fig. 6a).

408 Next, we investigated the effect of MV on regulation of *pmf* and g_H+ in WT *Arabidopsis* leaves. Upon
409 illumination of dark-adapted leaves, g_H+ was initially significantly higher in MV-treated WT leaves
410 than in control leaves (Fig. 6b), most likely due to dark-reduction of $AtCF_1\gamma$ by MV (Fig. 6a). As
411 illumination continued, g_H+ diminished in MV-treated leaves and remained at a very low level
412 throughout the rest of the experiment, even during HL (Fig. 6c). This results in very high *pmf* (Fig.
413 6d) and NPQ (Shapiguzov et al., 2020). In contrast, MV-treatment of *pgr5* mutant leaves caused only
414 a minor decrease in g_H+ and increase in *pmf* during illumination, and in HL g_H+ was in fact higher in
415 MV-treated *pgr5* mutant than in WT control leaves (Fig. 6c–d), suggesting that the MV-mediated g_H+
416 decrease is dependent on AtPGR5.

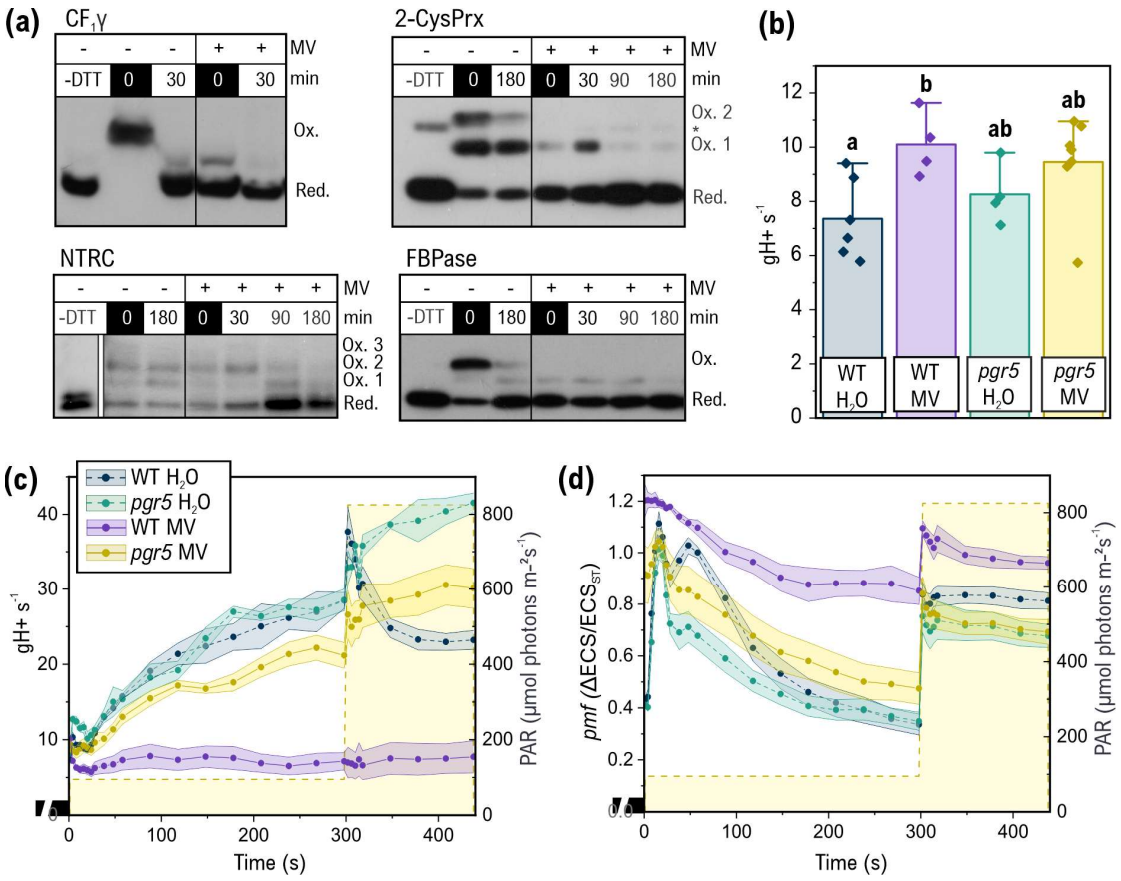

Figure 6. Effect of methyl viologen (MV) on thiol redox states of chloroplast enzymes and on regulation of *pmf* in *Arabidopsis*. (a) Mobility shift assays of AtCF$_1$γ, 2-CysPrxs, NTRC, and FBPase thiol redox state in vivo. WT Arabidopsis leaves were incubated in H_2O with (+) or without (-) 1 µM MV in dark and then illuminated in GL conditions for 180 min, with samples taken from darkness (0) and after 30, 90, and 180 min of illumination. Total protein extracts were labelled with MALPEG as described in Materials and Methods, separated by SDS-PAGE and probed with appropriate antibodies. MALPEG-labelled (in vivo oxidised) forms migrate more slowly than unlabelled forms (in vivo reduced). –DTT indicates control sample where no alkylation of thiols by MALPEG should occur, and * indicates dimeric 2CysPrx. **(b)** Conductivity of the thylakoid membrane (g_H+) after 1 s of illumination in growth light (GL, 95 µmol photons $m^{-2}s^{-1}$) in dark-adapted WT and *pgr5* mutant leaves incubated in H_2O with or without 1 µM MV. The values are mean + SD from 4–7 biological replicates. Statistical significance of differences was tested by one-way ANOVA and Tukey's tests ($p<0.05$). **(c)** Thylakoid conductivity and **(d)** *pmf* in dark-adapted WT and *pgr5* mutant leaves incubated in H_2O with or without 1 µM MV during 5 min illumination in GL (95 µmol photons $m^{-2}s^{-1}$) and consequent increase in light intensity to 825 µmol photons $m^{-2}s^{-1}$ (HL), as determined from dark-interval relaxation kinetics of the ECS signal. The values in C-D are averages from 4–7 biological replicates ± SEM (ribbon).

We also investigated the effect of perturbing the thiol redox state of the cell on thylakoid conductivity in *Synechocystis*. As moderate concentrations of MV have only minor effects on cyanobacterial electron transport (Sétif, 2015), with no significant impact on g_H+ observed after addition of 0.5 mM MV (Fig. S8), we opted to test the effect of supplementation with the thiol-alkylating agent N-ethylmaleimide (NEM). Addition of 0.1 mM NEM to WT *Synechocystis* cultures resulted in a significant increase in g_H+ after 5 seconds of illumination (Fig. 7a), similarly to results recently reported for another maleimide compound 2-methylmaleimide (Hubáček et al., 2024). In Δ*pgr5* cells,

only a slight, statistically non-significant NEM-induced increase in g_{H^+} was observed. In *Synechococcus*, which does not have PGR5, NEM did not have a significant effect on g_{H^+} (Fig. 7b). Finally, we also tested the effect of NEM on g_{H^+} in *Arabidopsis* WT and *pgr5* mutant leaves, repeating the fluctuating light experiment from Figure 1. NEM decreased g_{H^+} throughout the experiment in WT (Fig. 7c), albeit not as dramatically as MV treatment. In contrast, *pgr5* mutant leaves did not respond to NEM treatment during the first LL-HL cycle (Fig. 7c). During subsequent cycles g_{H^+} in NEM-treated *pgr5* mutant leaves decreased slightly in comparison to untreated *pgr5* mutant leaves, while still remaining higher than untreated WT leaves.

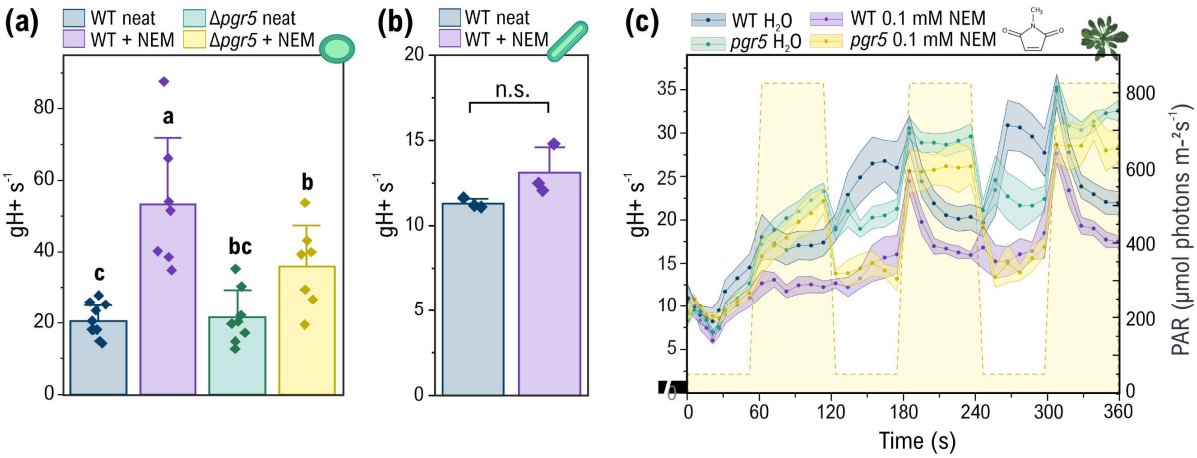

Figure 7. Effect of NEM on thylakoid conductivity under illumination. (a) The effect of 0.1 mM NEM on g_{H^+} in *Synechocystis* WT and Δ*pgr5* cells. ECS DIRK were measured 5 seconds after the onset of illumination at 500 µmol photons m^{-2} s^{-1}. The values are averages of 7–11 biological replicates + SD. Statistical significance of differences was tested by one-way ANOVA and Tukey's tests for comparison of means ($P<0.05$)**. (b)** The effect of 0.1 mM NEM on g_{H^+} in *Synechococcus elongatus* sp. PCC 7942 WT cells. ECS DIRK were measured as averaged decay kinetics from 5 dark intervals spaced 5 seconds apart, with the first DIRK being administered 5 seconds after the onset of illumination at 500 µmol photons m^{-2} s^{-1}. The values are averages of 3 biological replicates + SD. n.s. = statistically non-significant difference according to a paired *t*-test ($P=0.20$). **(c)** g_{H^+} was measured in *Arabidopsis* WT-gl1 and *pgr5* mutant leaves incubated on water or water + 0.1 mM NEM. The water samples are the same as in Figure 1, while the +NEM values are averages of 4 biological replicates ± SEM.

These results provided evidence that PGR5 is involved in a redox-dependent regulatory mechanism of ATP synthase activity that is distinct from $F_1\gamma$ redox state. Interestingly, it has been reported that PGR5 from cucumber (*Cucumis sativus L.*) can interact with the AtpB subunit of the chloroplast ATP synthase in yeast-two-hybrid tests (Wu et al., 2021)**.** To investigate the ability of PGR5 to directly interact with ATP synthase *in planta*, we performed bimolecular fluorescence complementation (BiFC) tests between AtPGR5 and $AtCF_1\gamma$. Indeed, strong YFP fluorescence co-localising with chlorophyll autofluorescence was detected, indicating interaction between the two proteins in chloroplast thylakoid membranes (Fig. 8a). As negative controls we performed BiFC tests between

467 AtPGR5 and the NdhS subunit of the chloroplast NAD(P)H dehydrogenase-like complex, another
468 major thylakoid protein complex, as well as $AtCF_1\gamma$ and Thioredoxin x, a chloroplast protein similar
469 in size to AtPGR5 (Fig. S9). Moreover, an Alphafold2 Multimer model predicts that SynPgr5 can
470 bind to the $F_1\gamma$ subunit of the *Synechocystis* ATP synthase (Fig. 8b). As the $F_1\varepsilon$-subunit likely remains
471 bound to $F_1\gamma$ even in its non-inhibitory conformation (Kato et al., 1997), we also included $F_1\varepsilon$ in our
472 model.

473

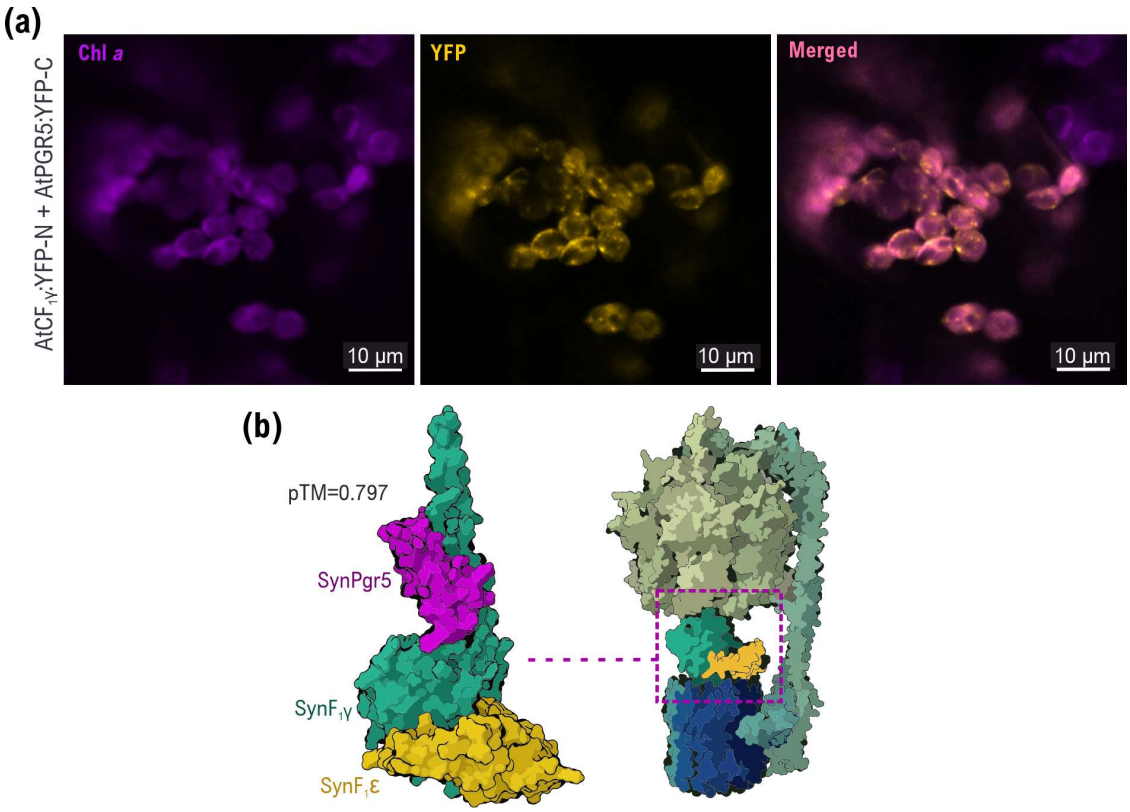

474

475 **Figure 8. Protein–protein interaction between ATP synthase and PGR5. (a)** Bimolecular fluorescence complementation
476 (BiFC) test for protein-protein interaction between Arabidopsis $CF_1\gamma$ fused to an N-terminal fragment of yellow fluorescent
477 protein ($AtCF_1\gamma$:YFP-N) and Arabidopsis PGR5 fused to a C-terminal YFP fragment (AtPGR5:YFP-C) in tobacco leaves.
478 The left panel shows Chlorophyll *a* autofluorescence in purple, the middle panel YFP fluorescence in yellow, and the right
479 panel a merged image of YFP and chlorophyll images. The scale bar is 10 µm. **(b)** An Alphafold2 Multimer prediction of an
480 interaction complex between *Synechocystis* ATP synthase γ subunit (*sll1327*, green), ATP synthase ε subunit (*slr1330,*
481 yellow*)*, and *Synechocystis* Pgr5 (*ssr2016*, magenta). The top-ranked model with a pTM score of 0.797 and an ipTM score of
482 0.702 is shown. Structure of a full Spinach chloroplast ATP synthase ($SoCF_0CF_1$) (Hahn et al., 2018) is shown for reference,
483 with the $CF_1\gamma$ and $CF_1\varepsilon$ subunits highlighted in green and yellow, respectively.

484

485 **DISCUSSION**

486 Substantial adjustments of thylakoid conductivity take place during sudden changes in light intensity
487 in both chloroplasts and cyanobacteria, in order to control induction of the photoprotective
488 mechanisms. Results shown herein indicate that this regulation is independent of the thiol redox state
489 of $CF_1\gamma$ (Fig. 1), but dependent on another redox-based mechanism that involves the PGR5 protein
490 (Fig. 6, Fig. 7) in a manner that has been conserved in evolution from free-living cyanobacteria to
491 green algae and C_3 plants, as well as C_4 plants.

492

493 **PGR5 has an evolutionarily conserved role in regulation of thylakoid conductivity**

494 The PGR5 protein has been previously understood to either directly catalyse or facilitate CET around
495 PSI in plants (Munekage et al., 2002) and cyanobacteria (Yeremenko et al., 2005). Lack of PGR5
496 caused a distinct inability to oxidise PSI in chloroplasts, which was interpreted as being caused by
497 failure to induce photosynthetic control and NPQ due to insufficient acidification of the thylakoid
498 lumen in the absence of PGR5-mediated CET (Yamamoto & Shikanai, 2019). However, contrasting
499 evidence was already provided early on showing that ferredoxin-dependent CET does function in the
500 absence of PGR5 (Nandha et al., 2007), suggesting that the phenotype of the *pgr5* mutant may be
501 caused by another mechanism.

502 We showed previously that in *pgr5 Arabidopsis* plants overexpressing the chloroplast NADPH-
503 dependent thioredoxin reductase (OE-NTRC *pgr5*), *pmf* was restored to a WT-level during LL-to-HL
504 transitions (Nikkanen et al., 2018). This was insufficient however, to induce photosynthetic control,
505 resulting in the OE-NTRC *pgr5* plants suffering from almost as severe over-reduction of the electron
506 transport chain as *pgr5* plants. Concurring results were more recently reported from *Arabidopsis*
507 plants expressing Plastid terminal oxidase 2 from *Chlamydomonas reinhardtii* (CrPTOX2) in the *pgr5*
508 mutant background: The introduction of CrPTOX2 resulted in restoration of WT-like (ΔpH-
509 dependent) NPQ, but oxidation of PSI was still as impaired as in *pgr5* mutants (Zhou et al., 2023).
510 These results suggest that the inability of *pgr5* mutants to induce photosynthetic control in HL is not
511 simply caused by loss of ΔpH, but the AtPGR5 protein is directly required. Similarly to *pgr5*, OE-
512 NTRC *pgr5* plants still showed elevated g_{H^+} during transitions to HL (Nikkanen et al., 2018). These
513 findings argue for a complex role of AtPGR5 in regulation of thylakoid proton conductivity and
514 electron transport.

515 The *Synechocystis* Δ*pgr5* mutant showed no impairment of CET (Fig. 3a). Our data is in line with a
516 study by Miller et al. showing that the antimycin a-sensitive pathway (=PGR5-dependent) does not
517 contribute to *pmf* formation during dark/light transitions in *Synechocystis*. Instead, the CET-dependent
518 fraction of *pmf* generation was entirely attributable to the NDH-1 complex (Miller et al., 2021). As the
519 extra ATP produced by CET is understood to enable more efficient operation of the CBC by adjusting

520 the ATP:NADPH ratio, the fact that no impairment of CO_2 fixation rate was observed in Δ*pgr5* (Fig.
521 4f) further indicates that SynPgr5 is not needed for CET in *Synechocystis.*

522 Our ECS results both with the *Chlamydomonas pgr5* mutant (Fig. 3c) as well as the *pgr5-Cas*
523 *Arabidopsis* mutant (Fig. S1C) showed elevated proton flux (v_H+) in HL, which is also incompatible
524 with a significant role for PGR5 in CET, and may rather indicate enhancement of the CET rate.
525 Accordingly, CrPGR5 was not detected in CET supercomplexes (Iwai et al., 2010). It was also
526 recently reported, based on simultaneous near-infrared and chlorophyll fluorescence spectroscopy,
527 that the absence of AtPGR5 enhanced CET activity in *Arabidopsis* (Maekawa et al., 2024). A lower
528 v_H+ in LL that cannot be fully explained by a lower linear electron transport rate has, however, been
529 reported in *Arabidopsis* (Degen et al., 2023) and *S. viridis* (Fig. S7) (Woodford et al., 2024) *pgr5*
530 mutants. Interestingly though, the *Arabidopsis pgr5-Cas* mutant showed WT-like v_H+ in LL (Fig.
531 S1c), suggesting that the low v_H+ in the *pgr5-1* mutant (Fig. S2a) may be affected by the additional
532 mutation of the At2g1724 gene (Wada et al., 2021).

533 If PGR5 was directly involved in ferredoxin-dependent CET, one would expect *pgr5* mutants to suffer
534 from a bottleneck of electron transfer at ferredoxin. It was recently shown that the Arabidopsis *pgr5*
535 mutant accumulates PSI centres with damaged FeS clusters, which results in an inability to reduce
536 Fed (Tiwari et al., 2024), meaning that the bottleneck likely forms already at P700. The accumulation
537 of damaged PSI centres makes it appear as if the mechanism of ferredoxin-dependent CET itself is
538 impaired. These results suggest that the phenotype of *pgr5* mutants may not be caused by direct
539 impairment of CET.

540

541 **PGR5-mediated downregulation of ATP synthase depends on thiol redox conditions**

542 The elevated g_H+ of PGR5-deficient *Synechocystis*, *Chlamydomonas*, *Arabidopsis,* and *S. viridis*
543 during high-light phases of fluctuating light (Fig. 1, Fig. 2, Fig. 4, Fig. S7) is consistent with PGR5
544 functioning as a direct or indirect down-regulator of ATP synthase activity (Kanazawa et al., 2017;
545 Nikkanen et al., 2018; Tikkanen et al., 2015). *In planta* interaction of AtPGR5 with $AtCF_1\gamma$ in BiFC
546 tests (Fig. 7a) and *in silico* modelling of SynPgr5-$SynF_1\gamma$- $SynF_1\varepsilon$ interaction complex (Fig. 8b)
547 suggest that PGR5 may inhibit ATP synthase by directly binding to the $F_1\gamma$ subunit. $F_1\varepsilon$-inhibition
548 likely prevents ATP hydrolysis in dark and LL conditions, when *pmf* is low, while PGR5 would limit
549 ATP synthase activity in HL, possibly allowed by the non-inhibitory "down" conformation of $F_1\varepsilon$
550 (Feniouk et al., 2010), to allow build-up of sufficient ΔpH for induction of photoprotection.

551 Moreover, this mechanism may be regulated by the thiol redox state of the chloroplast stroma or cell.
552 PGR5 contains a conserved cysteine residue (Munekage et al., 2002; Yeremenko et al., 2005), and

553 which could be target for regulatory thiol modifications. In line with this hypothesis, AtPGR5 was
554 found able to interact with AtNTRC in an *in planta* BiFC test, and overexpression of AtNTRC
555 resulted in intensified downregulation of thylakoid proton conductivity during transitions to HL, but
556 only in the presence of AtPGR5 (Nikkanen et al., 2018). Moreover, using a *pgr5 ntrc* double mutant
557 of *Arabidopsis*, Naranjo et al. showed that the high NPQ observed in *ntrc* mutant plants is dependent
558 on the presence of AtPGR5 (Naranjo et al., 2021). *Ntrc* mutant plants have a diminished AtPGR5
559 protein level (Nikkanen et al., 2018), most likely to compensate for the impaired activation of ATP
560 synthase via reduction of the $AtCF_1\gamma$ disulphide (Carrillo et al., 2016; Nikkanen et al., 2016).

561 It has been suggested that a disulphide bridge between AtPGR5 and AtPGRL1 is required for
562 PGR5/PGRL1-dependent CET in *Arabidopsis* (Hertle et al., 2013). However, a CrPGR5 with the
563 conserved cysteine residue mutated to a serine was able to complement the impairment of CET in the
564 *Chlamydomonas pgr5* mutant (Buchert et al., 2020), suggesting that the conserved cysteine residue in
565 PGR5 may be involved in a non-CET related regulatory mechanism.

566 Transient reduction of AtPGRL1 occurs upon onset of illumination, coinciding with increase in *pmf*,
567 PSI oxidation, and induction of NPQ (Chaturvedi et al., 2024; Hertle et al., 2013; Nikkanen et al.,
568 2018; Wolf et al., 2020). TRXm4 forms a disulphide bridge with AtPGRL1, and cleavage of that
569 disulphide (most likely by another thioredoxin isoform) and transient release of TRXm4 also occur at
570 dark-to-light transitions (Okegawa & Motohashi, 2020). This has been suggested to indicate activation
571 of CET (Chaturvedi et al., 2024; Hertle et al., 2013; Okegawa & Motohashi, 2020; Wolf et al., 2020),
572 but the same results could also be interpreted as reduction of AtPGRL1 affecting the association of
573 AtPGR5 with AtPGRL1, releasing AtPGR5 to interact with ATP synthase and to downregulate its
574 activity. This would limit H^+ efflux from the lumen and cause build-up of *pmf,* and consequently,
575 induction of NPQ and photosynthetic control. We therefore suggest that the phenotypes of *pgr5*
576 mutants may have been misinterpreted as being caused by directly impaired CET. For example, it was
577 recently shown that point mutations of disulphide-forming cysteine residues in AtPGRL1a results in
578 elevated *pmf*, NPQ, and donor-side limitation of PSI (Chaturvedi et al., 2024). While the authors did
579 not show data on g_{H^+}, it is possible that this phenotype was caused not by increased CET, but by
580 constitutive inhibition of ATP synthase activity by AtPGR5. Similarly, it has been reported that
581 AtPGR5 can enhance CET if both AtPGRL1 and AtPGRL2, a protein causing degradation of AtPGR5
582 in the absence of AtPGRL1, are missing (Rühle et al., 2021). This conclusion was based on higher
583 *pmf* and NPQ in the *pgrl1a pgrl1b pgrl2* triple mutant compared to *pgrl1* or *pgr5* single mutants. We
584 suggest, however, that the increased *pmf* was, again, probably mediated or at least contributed to by
585 lowered ATP synthase conductivity.

586 In the current study, we explored the effects of perturbing the chloroplast or cellular redox state agents
587 on the conductivity of ATP synthase. Interestingly, we found that addition of methyl viologen (MV)

588 results in strong reduction of chloroplast enzymes in *Arabidopsis*, including $AtCF_1\gamma$ (Fig. 6a).
589 Accordingly, g_H+ was elevated in dark-adapted MV-treated leaves (Fig. 6b). However, strong
590 downregulation of g_H+ during illumination was measured in MV-leaves, but only in the presence of
591 AtPGR5 (Fig. 6c). Thiol-alkylating agent N-ethylmaleimide (NEM) had a similar albeit less dramatic
592 effect (Fig. 7c). Interestingly, lack of AtPGR5 made the plants immune to NEM-induced g_H+ decrease
593 under HL, but did not prevent the decrease observed under LL phases of the fluctuating light
594 experiment. These results provide further evidence that AtPGR5 is required for redox-dependent
595 downregulation of g_H+ under high irradiance. We hypothesise that in WT *Arabidopsis*, addition of
596 MV likely causes strong reduction of either AtPGR5/AtPGRL1/AtTRXm4 directly or some
597 associated factor that would, without an MV treatment, function as an inhibitor of the ATP synthase
598 during sudden increases in light intensity. Importantly, this inhibitory effect overrides the activating
599 effect of a fully reduced $AtCF_1\gamma$. In the absence of AtPGR5, the inhibitory mechanism does not
600 function even in presence of MV.

601 We cannot fully exclude the possibility of the apparent reduction of chloroplast enzymes in presence
602 of MV being caused by overoxidation of thiols to sulphenic acids (Huang et al., 2019), especially in
603 the case of 2CysPRXs (Cerveau et al., 2016; Puerto-Galan et al., 2013). S-sulphenylated proteins
604 cannot form disulphides and thus cannot be labelled by the alkylating agent in our protocol, migrating
605 similarly to fully reduced proteins in mobility shift assays. Apart from 2CysPrxs, where the thiols are
606 required for the catalytic activity of the enzyme, overoxidation may in fact result in in a conformation
607 that is functionally similar to the reduced state of the protein. However, the elevation of g_H+ at the
608 onset of illumination in MV-treated leaves (Fig. 6b) suggests otherwise, at least in the case of $CF_1\gamma$ in
609 darkness. Moreover, overoxidation would inactivate 2-CysPRXs, preventing their oxidising effect on
610 other thiol proteins in the chloroplast, including $AtCF_1\gamma$ (Pérez-Ruiz et al., 2017; Vaseghi et al.,
611 2018). Similar results obtained with addition of NEM also make this scenario unlikely.

612 In *Synechocystis*, addition of NEM caused an opposite phenotype to *Arabidopsis*, with g_H+ being
613 elevated rather than diminished (Fig. 7a). The NEM-induced g_H+ increase was diminished in
614 *Synechocystis Δpgr5* and absent in WT *Synechococcus*, a species that does not have a PGR5
615 orthologue (Shimakawa et al., 2016). Untreated *Synechococcus* did, however, exhibit similar
616 downregulation of g_H+ under strong illumination as *Synechocystis* or *Arabidopsis* (Fig. S6). These
617 results suggest that the regulatory mechanisms involved in this response may differ between
618 organisms in terms of directionality of redox-regulation and involvement of PGR5, with
619 *Synechococcus* possibly using an unrelated, convergently evolved analogous mechanism. The
620 molecular details of these differing responses remain to be elucidated in future studies.

621 Interestingly, it has been reported that alkylation of cysteine 89 in the (*Spinacia oleracea*) $SoCF_1\gamma$ by
622 NEM or crosslinking Cys89 with Cys322 inhibits photophosphorylation and induces loss of the

623 proton gradient (Evron & Pick, 1997; McCarty & Fagan, 1973; Soteropoulos et al., 1994). This effect
624 was not observed in the dark, suggesting Cys89 only becomes accessible to modifications in light
625 upon generation of ΔpH (McCarty & Fagan, 1973). It is therefore possible that Cys89 is responsible
626 for the middle band in the At$CF_1\gamma$ mobility shift assays that is also present in the control sample (Fig.
627 1e), where all thiols accessible in the dark are alkylated with NEM before addition of MAL-PEG.
628 MAL-PEG likely gains access to Cys89 after the subsequent DTT treatment, resulting in the observed
629 mobility shift. The $F_1\gamma$ Cys89 residue is conserved in the green lineage, including cyanobacteria
630 (Hisabori et al., 2013), suggesting a functional role. Our Alphafold2 model of a Syn$F_1\gamma$-SynPGR5
631 interaction complex predicts, however, that neither the conserved Cys30 in SynPgr5 or Cys90 in
632 SynF1γ are involved in mediating the protein-protein interaction. This is also consistent with the lack
633 of changes in At$CF_1\gamma$ redox state in fluctuating light (Fig. 1e), suggesting that thiol/disulphide
634 exchanges of $F_1\gamma$ are not involved in the mechanism of adjusting g_H+ in fluctuating light. The
635 predicted binding of SynPgr5 to Syn$F_1\gamma$ in our model somewhat resembles the binding of the
636 inhibitory IF_1 protein to mitochondrial ATP synthase, which slots between the $F_1\gamma$, $F_1\alpha$, and $F_1\beta$
637 subunits (García-Bermúdez & Cuezva, 2016). This could also explain the observed interaction between
638 cucumber PGR5 and $F_1\beta$ (Wu et al., 2021).

639 An alternative or additional mechanism for the regulation of g_H+ in fluctuating light in plants could
640 function through changes in intercellular inorganic carbon concentration (C_i). C_i increases upon HL to
641 LL transitions as carbon fixation rate suddenly drops (Vialet-Chabrand et al., 2017), and increase in C_i
642 is known to increase g_H+ via an unknown regulatory pathway (Kohzuma et al., 2013). It is unlikely,
643 however, that the inability of *pgr5* to down-regulate g_H+ in HL would be caused by an elevated
644 concentration of C_i, because WT-like levels of C_i were measured under HL in PGR5-deficient rice
645 plants (Nishikawa et al., 2012). The carbon fixation capacity of *pgr5* plants only goes down as a
646 consequence of prolonged HL exposure and ensuing PSI photoinhibition (Gollan et al., 2017; Lima-
647 Melo et al., 2018). Similarly, we detected no impairment of CO_2 fixation in the *Synechocystis* Δ*pgr5*
648 mutant (Fig. 3F). Interestingly, expression of FlvA and FlvB from the moss *Physcomitrium patens* in
649 the *Arabidopsis pgr5* mutant background alleviated the elevated g_H+ phenotype (Yamamoto &
650 Shikanai, 2020), highlighting the complex relationship between oxidation of PSI and regulation of
651 ATP synthase.

652

653 **Physiological significance of PGR5-mediated downregulation of ATP synthase in *Synechocystis***

654 Lack of SynPgr5 caused no impairment of PSI oxidation or growth despite lowered *pmf* in
655 *Synechocystis* under fluctuating light (Fig. 2, Fig. 3b). This may be due to prevalence of FDPs as a
656 protective electron sink on the acceptor side of PSI in cyanobacteria (Allahverdiyeva et al., 2013;

657 Santana-Sanchez et al., 2019). Even in the absence of Flv1/3-mediated O_2 photoreduction in the
658 Δ*pgr5 flv3* double mutant, however, no significant additional impairment of PSI oxidation in
659 comparison to Δ*flv3* single mutant was observed (Fig. 2d–E). Slightly elevated FDP activity was
660 however measured in fluctuating light grown Δ*pgr5* under fluctuating light (Fig. 5), which may allow
661 the mutant to maintain sufficient PSI oxidation in HL despite diminished *pmf* and to grow similarly to
662 WT in fluctuating light (Fig. 2F). We have recently proposed that dissipation of *pmf* (lower cytosolic
663 pH) causes FDP hetero-oligomers to associate more strongly with the thylakoid membrane, increasing
664 photoprotective O_2 photoreduction activity (Eckardt et al., 2024; Nikkanen et al., 2023). In Δ*pgr5,* the
665 decreased *pmf* due to elevated g_H+ in HL (Fig. 2a) may therefore cause the slightly increased FDP
666 activity during the HL phases of fluctuating light conditions (Fig. 5), at least partly compensating for
667 the loss of photoprotective capacity via ΔpH-induced photosynthetic control.

668 Interestingly, there appears to be a regulatory link between FDPs, ATP synthase, and SynPgr5 in
669 cyanobacteria. During transitions to HL, lack of Flv1/3 results in a loss up to 75% of the proton flux
670 during the first minute of illumination in *Synechocystis* (Nikkanen et al., 2020) (Fig. S2b) as well as in
671 the filamentous model cyanobacterium *Anabaena* sp. PCC 7120 (Santana-Sánchez et al., 2023).
672 However, cyanobacterial cells compensate for this by downregulating g_H+ (Fig. 2a), achieving WT-
673 like *pmf* levels after the initial stages of HL transitions (Fig. 2b). In in the absence of both Flv1/3 and
674 SynPgr5 in the *Δpgr5 flv3* double mutant, however, this downregulation of g_H+ did not occur,
675 indicating that SynPgr5-mediated inhibition of ATP-synthase is required for the compensatory
676 mechanism. Interestingly, proton flux also recovered to WT-levels in *Δpgr5 flv3* (Fig. S2b),
677 suggesting e.g. increased CET via NDH-1.

678 It remains to be investigated what the environmental conditions are where SynPgr5 has a
679 physiologically significant role. Future studies should focus for example on mixotrophic conditions,
680 where overexpression of SynPgr5 has been shown to inhibit growth (Margulis et al., 2020) and
681 diurnal rhythms, which present additional challenges for coordination of the bioenergetic pathways
682 and metabolism in cyanobacteria (Ortega-Martínez et al., 2024; Solymosi et al., 2020).

683

684 **Conclusion**

685 The activity of chloroplast or cyanobacterial ATP synthase is dynamically regulated during
686 fluctuations in light intensity. These adjustments are not dependent on the thiol redox state of the $F_1\gamma$
687 subunit, but instead depend on the PGR5 protein as well as the thiol redox state of the stroma or
688 cytosol. This mechanism has been conserved in evolution from free-living cyanobacteria to
689 chloroplasts in algae, C_3 plants as well as C_4 plants. The inability to downregulate ATP synthase
690 activity under strong illumination is the only phenotype of PGR5-deficient knockout mutants that can

691 be observed in all representatives of the groups of photosynthetic organisms studied here;
692 cyanobacterium *Synechocystis* sp. PCC 6803, green alga *Chlamydomonas reinhardtii*, C_3 plant
693 *Arabidopsis thaliana*, and C_4 plant *Setaria viridiis*. The role of PGR5 is vital for oxidation of PSI in
694 plants and algae, but not in cyanobacteria. We also demonstrated that the cyanobacterial Pgr5 is not
695 needed for cyclic electron transport. We suggest that PGR5 directly binds to ATP synthase and
696 functions an inhibitory factor in a manner that is dependent on the thiol redox state of the cell or
697 chloroplast. The observed effect of plant PGR5 on CET is likely an indirect consequence of
698 misregulation of ATP synthase and, as shown by (Tiwari et al., 2024), increased photoinhibition of
699 PSI, although a role for PGR5 in regulating CET via Cyt b_6f cannot be excluded (Buchert et al.,
700 2020). Our study lays important groundwork for understanding the regulatory mechanisms of the *pmf*
701 and their evolution, possibly enabling biotechnologies to modulate *pmf* regulation for enhancement of
702 photosynthetic efficiency in crop plants or microbial bioproduction platforms.

703

704 **MATERIALS AND METHODS**

705 **Strains, plant lines and growth conditions**

706 *Arabidopsis thaliana* WT-gl1 or WT-Col-0, *pgr5-1* (At2g05620 knockout) (Munekage et al., 2002),
707 and *pgr5-Cas* (At2g05620 CRISPR-Cas9 mutant line) (Penzler et al., 2022) plants were grown for 4
708 weeks under 200 µmol photons in a 12/12h photoperiod before collecting individual leaves for
709 experiments.

710 For the BiFC experiments, WT *Nicotiana benthamiana* plants were grown under 130 µmol photons
711 m^{-2} s^{-1} at 23°C in a 16/8 hr light/dark photoperiod.

712 *Chlamydomonas reinhardtii* WT 137c, *pgr5* knockout and PGR5C complementation strains (Johnson
713 et al., 2014; Jokel et al., 2018) were grown under continuous 30 µmol photons m^{-2} s^{-1} at 25 °C and 120
714 rpm in TAP medium.

715 *Setaria viridis cv* MEO V34-1 *pgr5* knock-out mutant was generated using CRISPR-Cas9 gene-
716 editing as described in detail in (Ermakova et al., 2024). WT plants and plants with *pgr5-3* null alleles
717 described in (Woodford et al., 2024) were analysed. Plants were grown in a controlled environment
718 room with a 16 h : 8 h, light : dark photoperiod, 28°C day and 22°C night, 60% humidity and ambient
719 CO_2 at a light intensity of 300 µmol m^{-2} s^{-1} supplied by 1000 W red sunrise 3200K lamps (Sunmaster
720 Growlamps, Solon, OH, USA). Youngest fully expanded leaves of 3–4-week-old plants were used in
721 analysis.

722 *WT, Δpgr5, Δflv3* (Helman et al., 2003) and Δ*pgr5 flv3 Synechocystis* sp. PCC 6803 strains as well as
723 WT *Synechococcus elongatus* sp. PCC 7942 cells were grown under continuous 50 µmol photons m^{-2}
724 s^{-1} at 30 °C and air-level [CO_2] in pH 7.5 BG-11 medium. Unless stated otherwise, cultures were
725 grown for 4 days in 30 ml flasks, then pelleted and resuspended in fresh BG-11 at an appropriate
726 chlorophyll concentration for each experiment. For the growth curves under fluctuating light, WT,
727 *Δpgr5* and *Δpgr5 flv3* cells were grown for 7 days in conditions where light intensity was held at 20
728 µmol photons $m^{-2}s^{-1}$ and increased to 500 µmol photons $m^{-2}s^{-1}$ for 30 sec every 5 min. Samples were
729 taken and $OD_{750\ nm}$ measured with a spectrophotometer every 24h. For Fig. 5, cells were grown in a
730 regime in which light intensity fluctuated between 1 min periods of 25 and 500 µmol photons $m^{-2}s^{-1}$.

731

732

733 **Construction of Δ*pgr5* and Δ*pgr5 flv3* knockout mutants**

734 The upstream and downstream flanking sequences of the *pgr5* (*ssr2016*) gene and the *aphI* (Km^R)
735 gene replacing the *ssr2016* open reading frame were amplified from genomic DNA of Δ*pgr5* mutant
736 generated earlier in a different *Synechocystis* WT background as described in (Allahverdiyeva et al.,
737 2013). After transformation into *Synechocystis* sp. PCC 6803 WT strain and the Δ*flv3* strain (Helman
738 et al., 2003), the transformants were selected on BG-11 plates with 50 µg/ml kanamycin. Complete
739 segregation of the mutation was confirmed by PCR with specific forward primer 5′-
740 AGCCAAACCGCATCTAACG-3′ and reverse primer 5′-TTCATAACGCCTCCGGTC-3′. The
741 expected PCR fragment length was 0.7 kb for the WT and 1.7 kb for the mutant (Fig. S10). The
742 mutation in the *flv3* open reading frame was confirmed by using forward primer 5′-
743 GTACGGCATGTTCACTACC-3′ and reverse primer 5′- GATCAGCGTTAGCCTGTAA-3′, and the
744 expected PCR fragment length was 1.0 kb for the WT and 2.6 kb for the mutant (Fig. S10). Two
745 separate clones of Δ*pgr5* were used interchangeably for the experiments, as no difference was
746 detected in their phenotypes.

747

748 **Electrochromic shift (ECS) measurements**

749 Individual *Arabidopsis* leaves were measured with the Dual-PAM 100 spectrophotometer (Walz) and
750 its P515/535 accessory module (Schreiber & Klughammer, 2008) as described earlier (Guinea Diaz et
751 al., 2020; Nikkanen et al., 2018). For the experiment in Figure 1, dark-adapted (30 min) leaves were
752 exposed to a light regime fluctuating between 1 min periods of 50 and 825 µmol photons m^{-2} s^{-1}, with
753 250 ms dark intervals administered every 5 seconds for the first 30 seconds and every 10 seconds
754 thereafter. For the methyl viologen (MV) experiment, detached leaves were dark-incubated overnight

755 on water with 0.05% Tween-20 ± 1 µM MV. In the ECS measurement, dark intervals of 450 ms were
756 administered every 4 s until 28 s during 95 µmol photons $m^{-2}s^{-1}$ of actinic illumination, every 10 s
757 between 28 and 58 s, every 30 s between 58 and 298 s, every 4 s after transition to 825 µmol photons
758 $m^{-2}s^{-1}$ between 298 and 318 s, and every 30 s thereafter. 2,000 Hz pulse frequency of the measuring
759 light was used. ΔECS_T values were normalised to the ΔECS measured upon a single-turnover
760 saturating flash on dark-adapted leaves (ΔECS_{ST}) (Mathiot & Alric, 2021). For the NEM experiment,
761 detached leaves were incubated in dark on water with 0.05% Tween-20 ±0.1 mM NEM for 2 hours
762 before the experiment.

763 *Chlamydomonas* cultures were measured using the same protocol as *Arabidopsis*, with chlorophyll
764 concentration set to 20 µg/ml. Dark-adapted *S. viridis* leaves were subjected first to 15 min at 400
765 µmol photons m^{-2} s^{-1} and then to 10 min cycles at irradiance alternating between 2000 and 400 µmol
766 photons m^{-2} s^{-1}. The actinic light was switched off for 30 s at 2 min since the beginning of
767 illumination and then at 5 min intervals.

768 ECS changes were measured from *Synechocystis and Synechococcus* cells by monitoring the 500-480
769 nm absorbance difference signal (Viola et al., 2019) using a JTS-10 spectrophotometer (BioLogic) as
770 described in (Nikkanen et al., 2020). Cells were pelleted and resuspended in fresh BG-11 at 7.5 µg
771 Chl ml^{-1}. When appropriate, 0.1 mM NEM was added to the samples before a 5 min dark-adaption
772 prior to the measurement. Each measurement was also conducted with the cells illuminated only by
773 the measuring light flashes, and the ECS changes recorded were then subtracted from the
774 measurements under green actinic light, in order to control for any actinic effects of the measuring
775 light. A moderate (60 µmol photons m^{-2} s^{-1}, relative to growth light of 50 µmol) rather than a low
776 actinic light intensity was used in fluctuating light to allow a sufficient signal-to-noise ratio for DIRK
777 analysis. The cyanobacterial ECS signals were not normalised to ECS_{ST} due to a low signal-to-noise
778 ratio of single turnover traces. Instead, a constant chlorophyll concentration was used.

779 The *pmf* and g_H+ parameters were determined as the difference between magnitude of the ECS signal
780 in light – y0 value of a first-order fit to the decay kinetics of the signal during a dark interval, and the
781 inverse of the time constant of the fit, respectively, while v_H+ was derived as *pmf* x g_H+ (Cruz et al.,
782 2005). Fitting and data processing was done with the OriginPro 2024b (OriginLab) software.

783

784 **Saturating pulse analysis of chlorophyll fluorescence and $P700^+$**

785 The extents of the donor side and acceptor side limitations of PSI, Y(ND) and Y(NA), respectively,
786 were determined under fluctuating light conditions by a saturating pulse analysis of the $P700^+$ signal
787 using the Dual-PAM 100 (Klughammer & Schreiber, 2008). Chlorophyll autofluorescence was

788 simultaneously recorded to determine the Y(NPQ) parameter (in *Arabidopsis*) as described by
789 (Schreiber et al., 2008). Saturating pulses (8000 µmol photons m^{-2} s^{-1} for *Arabidopsis* and 3000 for
790 *Synechocystis*) were administered every 15 seconds during illumination.

791

792 **Deconvoluted P700, plastocyanin, and ferredoxin redox changes**

793 The deconvoluted plastocyanin (PC), P700, and ferredoxin redox changes were determined by NIR
794 absorbance difference spectroscopy using the DUAL-KLAS-NIR spectrophotometer (Walz)
795 (Klughammer & Schreiber, 2016). CET and LET at PSI in *Synechocystis* were quantified using
796 analysis of dark-interval relaxation kinetics (DIRK) according to (Theune et al., 2021) with
797 modifications. *Synechocystis* cells were pelleted and adjusted to 15 µg Chl ml^{-1} with fresh BG-11.
798 Cells were pre-illuminated for 2 min with 500µE, followed by administration of 100 dark intervals of
799 20 ms. The 100 decay traces were averaged and initial slopes of the PC and P700 decay curves were
800 used to calculate J_{PSI}. J_{PSI}-CET was determined by repeating the same experiment in the presence of
801 10µM DCMU to block electron transport from PSII. The NIRMAX script (Klughammer & Schreiber,
802 2016) modified for cyanobacteria was used to determine the maximal oxidation of PC and P700 and
803 maximal reduction of Fed. The model spectra for the deconvolution of PC, P700, and Fed redox
804 changes in *Synechocystis* were measured as described in (Nikkanen et al., 2020). Arabidopsis
805 NIRMAX measurements of dark-adapted leaves were conducted as described in (Nikkanen et al.,
806 2019). Reduction kinetics of Fed under far red light were measured after running the NIRMAX script,
807 illuminating detached leaves for 1 second with intensity 20 far-red light.

808

809 **Protein thiol alkylation and SDS-PAGE**

810 4-week-old *Arabidopsis* WT-Col-0 plants were dark-adapted, exposed to a light regime fluctuating
811 between 1-minute periods of 50 and 800 µmol photons. Samples (individual leaves) were taken every
812 20 seconds and quickly placed in 10% % TCA solution to freeze the thiol redox state of proteins.
813 TCA precipitation, alkylation of thiols with MALPEG-5000, and SDS-PAGE was then performed as
814 described in Nikkanen et al., (2016). Briefly, free thiol groups were first alkylated with NEM.
815 Following alkylation, disulphide bonds in proteins were reduced with dithiothreitol (DTT), and the
816 resulting thiols were then alkylated using methoxypolyethylene glycol maleimide Mn 5000 (MAL-
817 PEG, Sigma-Aldrich). This treatment makes the in-vivo oxidised forms of proteins migrate more
818 slowly than reduced ones in SDS-PAGE. For MV-treated samples, detached leaves were dark-
819 incubated overnight on water with 0.05% Tween-20 or water 0.05% Tween + 1 µM MV. Leaves were

820 then illuminated in growth conditions for 0, 30, 90, or 180 min before sample collection and
821 placement in 10% TCA.

822 Total protein extractions from *Synechocystis* cells were done as described in (Zhang et al., 2009), and
823 protein concentration was determined by the DC Protein Assay Kit (Bio-Rad, based on the Lowry
824 assay). Sodium dodecyl sulfate polyacrylamide gel electrophoresis (SDS-PAGE) and immunoblotting
825 were performed as previously described (Nikkanen et al., 2016). 4–15% Mini-PROTEAN TGX
826 precast gels (Bio-Rad) were used for electrophoresis except for Figure 5, for which 12%
827 polyacrylamide gels with 6M urea were cast. PVDF membranes were probed with antibodies raised
828 against $CF_1\gamma$ (Agrisera, AS08 312), FBPase (courtesy of Dr M. Sahrawy), AtpB (Agrisera, AS), Flv3
829 (Genscript), NTRC (Lepistö et al., 2009), or 2-CysPrx (courtesy of Prof. F. J. Cejudo).

830

831 **Membrane Inlet Mass Spectrometry (MIMS)**

832 *Synechocystis in vivo* O_2 and CO_2 gas fluxes were monitored in real-time by membrane inlet mass
833 spectrometry (MIMS) as described earlier (Mustila et al., 2016), with O_2 uptake distinguished from O_2
834 evolution by enrichment of the $^{18}O_2$ isotope in the medium. Chlorophyll concentration was set to 10
835 µg/ml, 1.5 mM $NaHCO_3$ was added, and cells were dark-adapted for 15 min prior to the
836 measurements. Gas exchange was monitored under 500 µmol photons $m^{-2}s^{-1}$ illumination for 5 min.
837 See legend for Fig. 3 for experimental details.

838

839 **Bimolecular Fluorescence Complementation (BiFC) tests**

840 *In planta* protein–protein interaction tests by bimolecular fluorescence complementation (BiFC) were
841 conducted as described earlier (Nikkanen et al., 2016, 2018). *Nicotiana benthamiana* plants were used
842 for transient expression of fusion constructs via *Agrobacterium tumefaciens* strain GV3101
843 infiltration. Imaging was done 3 days after infiltration using a Zeiss LSM780 confocal microscope.
844 Construction of the AtPGR5:YFP-C and AtNdhS:YFP-N expression vectors for YFP-fusion proteins
845 is described in (Nikkanen et al., 2018) and construction of the $AtCF_1\gamma$:YFP-N and AtTRXx:YFP-C
846 vectors in (Nikkanen et al., 2016).

847 ***In silico* modelling**

848 The amino acid sequences for *Synechocystis* genes *sll1327, slr1330* and *ssr2016* were retrieved from
849 the Uniprot database (entries P17253, P26533, and P73358, respectively). AlphaFold2 Multimer
850 Google Colab notebook (Mirdita et al., 2022) was used to model the interaction complex using 6
851 recycles and pdb100 template mode, with Amber relaxation of the best model. The model with the

best pTM score was selected for visualisation using the Mol* 3D viewer (Sehnal et al., 2021). The *Spinacia oleracea* chloroplast ATP synthase structure (Hahn et al., 2018) was retrieved from the RCSB PDB database (entry 6FKF) and visualised by Mol* 3D viewer.

Acknowledgements

We thank Dr. Martina Jokel and Darius Kosmützky for providing *Chlamydomonas* strains, and for assisting with *Chlamydomonas* cell culture, respectively. Linda Nevala, Mahfuzur Rahman, and Tapio Ronkainen are thanked for technical assistance, and the Turku Bioscience CIC Imaging Core for imaging infrastructure and assistance.

Funding

This work was supported by the Research Council of Finland grants #354876 (to L.N.), #315119 (to Y.A.), and # 276392 (to E.R.), funding from Jane and Aatos Erkko Foundation (to E.R.), Novo Nordisk Foundation grants NNF20OC0064371 (PhotoCat, to Y.A.) and NNF22OCOO79717 (Photo-e-Microbes, to L.T.W.) as well as Australian Research Council 's Discovery Project (DP230100175) and the Thomas Davies Research Grant for Marine, Soil and Plant Biology from the Australian Academy of Sciences (to M.E.).

Author Contributions

L.N. conceived the research idea, devised the experimental plan, performed most of the experiments, analysed the data, and wrote the first draft of the article. L.T.W. performed part of the cyanobacterial ECS and DKN measurements and analysed the data. R.W. and M.E. performed the ECS measurements in *S. viridis* and analysed the data. H.M. created the *Synechocystis* Δ*pgr5* and Δ*pgr5 flv3* mutants. E.R. and Y.A. supervised research and provided resources. All authors participated in editing the article.

References

Akiyama, K., Ozawa, S.-I., Takahashi, Y., Yoshida, K., Suzuki, T., Kondo, K., Wakabayashi, K., & Hisabori, T. (2023). Two specific domains of the γ subunit of chloroplast F_oF_1 provide redox

regulation of the ATP synthesis through conformational changes. *Proceedings of the National Academy of Sciences*, *120*(6). https://doi.org/10.1073/pnas.2218187120

Allahverdiyeva, Y., Mustila, H., Ermakova, M., Bersanini, L., Richaud, P., Ajlani, G., Battchikova, N., Cournac, L., & Aro, E.-M. (2013). Flavodiiron proteins Flv1 and Flv3 enable cyanobacterial growth and photosynthesis under fluctuating light. *Proceedings of the National Academy of Sciences of the United States of America*, *110*(10), 4111–4116. https://doi.org/10.1073/pnas.1221194110

Armbruster, U., Carrillo, L. R., Venema, K., Pavlovic, L., Schmidtmann, E., Kornfeld, A., Jahns, P., Berry, J. A., Kramer, D. M., & Jonikas, M. C. (2014). Ion antiport accelerates photosynthetic acclimation in fluctuating light environments. *Nature Communications*, *5*, 5439. https://doi.org/10.1038/ncomms6439

Armbruster, U., Correa Galvis, V., Kunz, H. H., & Strand, D. D. (2017). The regulation of the chloroplast proton motive force plays a key role for photosynthesis in fluctuating light. *Current Opinion in Plant Biology*, *37*, 56–62. https://doi.org/S1369-5266(17)30002-X [pii]

Avenson, T. J., Cruz, J. A., Kanazawa, A., & Kramer, D. M. (2005). Regulating the proton budget of higher plant photosynthesis. *Proceedings of the National Academy of Sciences of the United States of America*, *102*(27), 9709–9713. https://doi.org/10.1073/pnas.0503952102

Bailleul, B., Cardol, P., Breyton, C., & Finazzi, G. (2010). Electrochromism: a useful probe to study algal photosynthesis. *Photosynthesis Research*, *106*(1–2), 179–189. https://doi.org/10.1007/s11120-010-9579-z

Balmer, Y., Vensel, W. H., Hurkman, W. J., & Buchanan, B. B. (2006). Thioredoxin target proteins in chloroplast thylakoid membranes. *Antioxidants & Redox Signaling*, *8*(9–10), 1829–1834. https://doi.org/10.1089/ars.2006.8.1829

Buchert, F., Bailleul, B., & Joliot, P. (2021). Disentangling chloroplast ATP synthase regulation by proton motive force and thiol modulation in Arabidopsis leaves. *Biochimica et Biophysica Acta (BBA) - Bioenergetics*, *1862*(8), 148434. https://doi.org/10.1016/j.bbabio.2021.148434

Buchert, F., Mosebach, L., Gäbelein, P., & Hippler, M. (2020). PGR5 is required for efficient Q cycle in the cytochrome b6f complex during cyclic electron flow. *The Biochemical Journal*, *477*(9), 1631–1650. https://doi.org/10.1042/BCJ20190914 [doi]

Carraretto, L., Formentin, E., Teardo, E., Checchetto, V., Tomizioli, M., Morosinotto, T., Giacometti, G. M., Finazzi, G., & Szabo, I. (2013). A Thylakoid-Located Two-Pore K+ Channel Controls Photosynthetic Light Utilization in Plants. *Science*, *342*(6154), 114–118. https://doi.org/10.1126/science.1242113

Carrillo, L. R., Froehlich, J. E., Cruz, J. A., Savage, L. J., & Kramer, D. M. (2016). Multi-level regulation of the chloroplast ATP synthase: the chloroplast NADPH thioredoxin reductase C (NTRC) is required for redox modulation specifically under low irradiance. *Plant Journal*, *87*(6), 654–663. https://doi.org/10.1111/tpj.13226

Cerveau, D., Ouahrani, D., Marok, M. A., Blanchard, L., & Rey, P. (2016). Physiological relevance of plant 2-Cys peroxiredoxin overoxidation level and oligomerization status. *Plant Cell and Environment*, *39*(1), 103–119. https://doi.org/10.1111/pce.12596

Chaturvedi, A. K., Dym, O., Levin, Y., & Fluhr, R. (2024). PGR5-LIKE PHOTOSYNTHETIC PHENOTYPE1A redox states alleviate photoinhibition during changes in light intensity. *Plant Physiology*, *194*(2), 1059–1074. https://doi.org/10.1093/plphys/kiad518

Checchetto, V., Segalla, A., Allorent, G., La Rocca, N., Leanza, L., Giacometti, G. M., Uozumi, N., Finazzi, G., Bergantino, E., & Szabò, I. (2012). Thylakoid potassium channel is required for efficient photosynthesis in cyanobacteria. *Proceedings of the National Academy of Sciences*, *109*(27), 11043–11048. https://doi.org/10.1073/pnas.1205960109

Cobley, J., Noble, A., Bessell, R., Guille, M., & Husi, H. (2020). Reversible Thiol Oxidation Inhibits the Mitochondrial ATP Synthase in Xenopus laevis Oocytes. *Antioxidants*, *9*(3), 215. https://doi.org/10.3390/antiox9030215

Cruz, J. A., Avenson, T. J., Kanazawa, A., Takizawa, K., Edwards, G. E., & Kramer, D. M. (2005). Plasticity in light reactions of photosynthesis for energy production and photoprotection. *Journal of Experimental Botany*, *56*(411), 395–406. https://doi.org/10.1093/jxb/eri022

Cruz, J. A., Sacksteder, C. A., Kanazawa, A., & Kramer, D. M. (2001). Contribution of electric field (Delta psi) to steady-state transthylakoid proton motive force (pmf) in vitro and in vivo. Control of pmf parsing into Delta psi and Delta pH by ionic strength. *Biochemistry*, *40*(5), 1226–1237. https://doi.org/10.1021/bi0018741

DalCorso, G., Pesaresi, P., Masiero, S., Aseeva, E., Schuenemann, D., Finazzi, G., Joliot, P., Barbato, R., & Leister, D. (2008). A complex containing PGRL1 and PGR5 is involved in the switch between linear and cyclic electron flow in Arabidopsis. *Cell*, *132*(2), 273–285. https://doi.org/10.1016/j.cell.2007.12.028

Dann, M., & Leister, D. (2019). Evidence that cyanobacterial Sll1217 functions analogously to PGRL1 in enhancing PGR5-dependent cyclic electron flow. *Nature Communications*, *10*, 5299. https://doi.org/10.1038/s41467-019-13223-0

Davis, G. A., Kanazawa, A., Schoettler, M. A., Kohzuma, K., Froehlich, J. E., Rutherford, A. W., Satoh-Cruz, M., Minhas, D., Tietz, S., Dhingra, A., & Kramer, D. M. (2016). Limitations to photosynthesis by proton motive force-induced photosystem II photodamage. *Elife*, *5*, e16921. https://doi.org/10.7554/eLife.16921

Degen, G. E., Jackson, P. J., Proctor, M. S., Zoulias, N., Casson, S. A., & Johnson, M. P. (2023). High cyclic electron transfer via the PGR5 pathway in the absence of photosynthetic control. *Plant Physiology*, *192*(1), 370–386. https://doi.org/10.1093/plphys/kiad084

Degen, G. E., & Johnson, M. P. (2024). Photosynthetic control at the cytochrome *b* 6 *f* complex. *The Plant Cell*, *36*(10), 4065–4079. https://doi.org/10.1093/plcell/koae133

del Riego, G., Casano, L. M., Martin, M., & Sabater, B. (2006). Multiple phosphorylation sites in the beta subunit of thylakoid ATP synthase. *Photosynthesis Research*, *89*(1), 11–18. https://doi.org/10.1007/s11120-006-9078-4

Eckardt, N. A., Allahverdiyeva, Y., Alvarez, C. E., Büchel, C., Burlacot, A., Cardona, T., Chaloner, E., Engel, B. D., Grossman, A. R., Harris, D., Herrmann, N., Hodges, M., Kern, J., Kim, T. D., Maurino, V. G., Mullineaux, C. W., Mustila, H., Nikkanen, L., Schlau-Cohen, G., … Yano, J. (2024). Lighting the way: Compelling open questions in photosynthesis research. *The Plant Cell*. https://doi.org/10.1093/plcell/koae203

Ermakova, M., Woodford, R., Fitzpatrick, D., Nix, S. J., Zwahlen, S. M., Farquhar, G. D., von Caemmerer, S., & Furbank, R. T. (2024). Chloroplast NADH dehydrogenase-like complex-mediated cyclic electron flow is the main electron transport route in <scp>C</scp> $_4$ bundle sheath cells. *New Phytologist*, *243*(6), 2187–2200. https://doi.org/10.1111/nph.19982

Evron, Y., & Pick, U. (1997). Modification of Sulfhydryl Groups in the [gamma]-Subunit of Chloroplast-Coupling Factor 1 Affects the Proton Slip through the ATP Synthase. *Plant Physiology*, *115*(4), 1549–1555. https://doi.org/10.1104/pp.115.4.1549

Fan, D.-Y., Nie, Q., Hope, A. B., Hillier, W., Pogson, B. J., & Chow, W. S. (2007). Quantification of cyclic electron flow around Photosystem I in spinach leaves during photosynthetic induction. *Photosynthesis Research*, *94*(2–3), 347–357. https://doi.org/10.1007/s11120-006-9127-z

Feniouk, B. A., Kato-Yamada, Y., Yoshida, M., & Suzuki, T. (2010). Conformational Transitions of Subunit ε in ATP Synthase from Thermophilic Bacillus PS3. *Biophysical Journal*, *98*(3), 434–442. https://doi.org/10.1016/j.bpj.2009.10.023

Feniouk, B. A., Suzuki, T., & Yoshida, M. (2006). The role of subunit epsilon in the catalysis and regulation of FOF1-ATP synthase. *Biochimica et Biophysica Acta (BBA) - Bioenergetics*, *1757*(5–6), 326–338. https://doi.org/10.1016/j.bbabio.2006.03.022

Foyer, C. H., & Hanke, G. (2022). ROS production and signalling in chloroplasts: cornerstones and evolving concepts. *The Plant Journal*, *111*(3), 642–661. https://doi.org/10.1111/tpj.15856

Fujii, T., Yokoyama, E., Inoue, K., & Sakurai, H. (1990). The sites of electron donation of Photosystem I to methyl viologen. *Biochimica et Biophysica Acta (BBA) - Bioenergetics*, *1015*(1), 41–48. https://doi.org/10.1016/0005-2728(90)90213-N

García-Bermúdez, J., & Cuezva, J. M. (2016). The ATPase Inhibitory Factor 1 (IF1): A master regulator of energy metabolism and of cell survival. *Biochimica et Biophysica Acta (BBA) - Bioenergetics*, *1857*(8), 1167–1182. https://doi.org/10.1016/j.bbabio.2016.02.004

Gollan, P. J., Lima-Melo, Y., Tiwari, A., Tikkanen, M., & Aro, E.-M. (2017). Interaction between photosynthetic electron transport and chloroplast sinks triggers protection and signalling important for plant productivity. *Philosophical Transactions of the Royal Society B: Biological Sciences*, *372*(1730). https://doi.org/10.1098/rstb.2016.0390

Guinea Diaz, M., Nikkanen, L., Himanen, K., Toivola, J., & Rintamäki, E. (2020). Two chloroplast thioredoxin systems differentially modulate photosynthesis in Arabidopsis depending on light intensity and leaf age. *Plant Journal*, *104*(3). https://doi.org/10.1111/tpj.14959

Guo, J., Nguyen, A. Y., Dai, Z., Su, D., Gaffrey, M. J., Moore, R. J., Jacobs, J. M., Monroe, M. E., Smith, R. D., Koppenaal, D. W., Pakrasi, H. B., & Qian, W. J. (2014). Proteome-wide light/dark modulation of thiol oxidation in cyanobacteria revealed by quantitative site-specific redox proteomics. *Molecular & Cellular Proteomics : MCP*, *13*(12), 3270–3285. https://doi.org/10.1074/mcp.M114.041160 [doi]

Hahn, A., Vonck, J., Mills, D. J., Meier, T., & Kühlbrandt, W. (2018). Structure, mechanism, and regulation of the chloroplast ATP synthase. *Science*, *360*(6389). https://doi.org/10.1126/science.aat4318

Hangarter, R. P., & Good, N. E. (1982). Energy Thresholds for Atp Synthesis in Chloroplasts. *Biochimica et Biophysica Acta*, *681*(3), 397–404. https://doi.org/10.1016/0005-2728(82)90181-5

Helman, Y., Tchernov, D., Reinhold, L., Shibata, M., Ogawa, T., Schwarz, R., Ohad, I., & Kaplan, A. (2003). Genes encoding a-type flavoproteins are essential for photoreduction of O-2 in cyanobacteria. *Current Biology*, *13*(3), 230–235. https://doi.org/10.1016/S0960-9822(03)00046-0

Herdean, A., Nziengui, H., Zsiros, O., Solymosi, K., Garab, G., Lundin, B., & Spetea, C. (2016). The Arabidopsis Thylakoid Chloride Channel AtCLCe Functions in Chloride Homeostasis and Regulation of Photosynthetic Electron Transport. *Frontiers in Plant Science*, *7*, 115. https://doi.org/10.3389/fpls.2016.00115

Herdean, A., Teardo, E., Nilsson, A. K., Pfeil, B. E., Johansson, O. N., Unnep, R., Nagy, G., Zsiros, O., Dana, S., Solymosi, K., Garab, G., Szabo, I., Spetea, C., & Lundin, B. (2016). A voltage-dependent chloride channel fine-tunes photosynthesis in plants. *Nature Communications*, *7*, 11654. https://doi.org/10.1038/ncomms11654

Hertle, A. P., Blunder, T., Wunder, T., Pesaresi, P., Pribil, M., Armbruster, U., & Leister, D. (2013). PGRL1 Is the Elusive Ferredoxin-Plastoquinone Reductase in Photosynthetic Cyclic Electron Flow. *Molecular Cell*, *49*(3), 511–523. https://doi.org/10.1016/j.molcel.2012.11.030

Hirasawa, M., & Tamura, G. (1980). Ferredoxin-Dependent Nitrite Reductase from Spinach Leaves. *Agricultural and Biological Chemistry*, *44*(4), 749–758. https://doi.org/10.1080/00021369.1980.10864029

Hisabori, T., Sunamura, E.-I., Kim, Y., & Konno, H. (2013). The Chloroplast ATP Synthase Features the Characteristic Redox Regulation Machinery. *Antioxidants & Redox Signaling*, *19*(15), 1846–1854. https://doi.org/10.1089/ars.2012.5044

Huang, J., Willems, P., Wei, B., Tian, C., Ferreira, R. B., Bodra, N., Gache, S. A. M., Wahni, K., Liu, K., Vertommen, D., Gevaert, K., Carroll, K. S., Van Montagu, M., Yang, J., Van Breusegem, F., & Messens, J. (2019). Mining for protein S-sulfenylation in Arabidopsis uncovers redox-sensitive

sites. *Proceedings of the National Academy of Sciences of the United States of America*, *116*(42), 21256–21261. https://doi.org/10.1073/pnas.1906768116

Hubáček, M., Wey, L. T., Kourist, R., Malihan-Yap, L., Nikkanen, L., & Allahverdiyeva, Y. (2024). Strong heterologous electron sink outcompetes alternative electron transport pathways in photosynthesis. *The Plant Journal*. https://doi.org/10.1111/tpj.16935

Ilik, P., Pavlovic, A., Kouril, R., Alboresi, A., Morosinotto, T., Allahverdiyeva, Y., Aro, E.-M., Yamamoto, H., & Shikanai, T. (2017). Alternative electron transport mediated by flavodiiron proteins is operational in organisms from cyanobacteria up to gymnosperms. *New Phytologist*, *214*(3), 967–972. https://doi.org/10.1111/nph.14536

Imashimizu, M., Bernat, G., Sunamura, E.-I., Broekmans, M., Konno, H., Isato, K., Roegner, M., & Hisabori, T. (2011). Regulation of F0F1-ATPase from Synechocystis sp PCC 6803 by gamma and epsilon Subunits Is Significant for Light/Dark Adaptation. *Journal of Biological Chemistry*, *286*(30), 26595–26602. https://doi.org/10.1074/jbc.M111.234138

Iwai, M., Takizawa, K., Tokutsu, R., Okamuro, A., Takahashi, Y., & Minagawa, J. (2010). Isolation of the elusive supercomplex that drives cyclic electron flow in photosynthesis. *Nature*, *464*(7292), 1210–1213. https://doi.org/10.1038/nature08885

Johnson, X., Steinbeck, J., Dent, R. M., Takahashi, H., Richaud, P., Ozawa, S.-I., Houille-Vernes, L., Petroutsos, D., Rappaport, F., Grossman, A. R., Niyogi, K. K., Hippler, M., & Alric, J. (2014). Proton Gradient Regulation 5-Mediated Cyclic Electron Flow under ATP- or Redox-Limited Conditions: A Study of Ƌ *ATPase pgr5* and Ƌ *rbcL pgr5* Mutants in the Green Alga *Chlamydomonas reinhardtii* . *Plant Physiology*, *165*(1), 438–452. https://doi.org/10.1104/pp.113.233593

Jokel, M., Johnson, X., Peltier, G., Aro, E.-M., & Allahverdiyeva, Y. (2018). Hunting the main player enabling Chlamydomonas reinhardtii growth under fluctuating light. *Plant Journal*, *94*(5), 822–835. https://doi.org/10.1111/tpj.13897

Joliot, P., & Johnson, G. N. (2011). Regulation of cyclic and linear electron flow in higher plants. *Proceedings of the National Academy of Sciences of the United States of America*, *108*(32), 13317–13322. https://doi.org/10.1073/pnas.1110189108

Kanazawa, A., & Kramer, D. M. (2002). In vivo modulation of nonphotochemical exciton quenching (NPQ) by regulation of the chloroplast ATP synthase. *Proceedings of the National Academy of Sciences of the United States of America*, *99*(20), 12789–12794. https://doi.org/10.1073/pnas.182427499

Kanazawa, A., Ostendorf, E., Kohzuma, K., Hoh, D., Strand, D. D., Sato-Cruz, M., Savage, L., Cruz, J. A., Fisher, N., Froehlich, J. E., & Kramer, D. M. (2017). Chloroplast ATP Synthase Modulation of the Thylakoid Proton Motive Force: Implications for Photosystem I and Photosystem II Photoprotection. *Frontiers in Plant Science*, *8*, 719. http://journal.frontiersin.org/article/10.3389/fpls.2017.00719

Kato, Y., Matsui, T., Tanaka, N., Muneyuki, E., Hisabori, T., & Yoshida, M. (1997). Thermophilic F1-ATPase Is Activated without Dissociation of an Endogenous Inhibitor, ε Subunit. *Journal of Biological Chemistry*, *272*(40), 24906–24912. https://doi.org/10.1074/jbc.272.40.24906

Kiirats, O., Cruz, J. A., Edwards, G. E., & Kramer, D. M. (2009). Feedback limitation of photosynthesis at high CO2 acts by modulating the activity of the chloroplast ATP synthase. *Functional Plant Biology*, *36*(10–11), 893–901. https://doi.org/10.1071/FP09129

Klughammer, C., & Schreiber, U. (2008). Saturation Pulse method for assessment of energy conversion in PSI. *PAM Application Notes*, *1*, 11–14.

Klughammer, C., & Schreiber, U. (2016). Deconvolution of ferredoxin, plastocyanin, and P700 transmittance changes in intact leaves with a new type of kinetic LED array spectrophotometer. *Photosynthesis Research*, *128*(2), 195–214. https://doi.org/10.1007/s11120-016-0219-0 [doi]

Kohzuma, K., Dal Bosco, C., Meurer, J., & Kramer, D. M. (2013). Light- and Metabolism-related Regulation of the Chloroplast ATP Synthase Has Distinct Mechanisms and Functions. *Journal of Biological Chemistry*, *288*(18), 13156–13163. https://doi.org/10.1074/jbc.M113.453225

Kohzuma, K., Froehlich, J. E., Davis, G. A., Temple, J. A., Minhas, D., Dhingra, A., Cruz, J. A., & Kramer, D. M. (2017). The Role of Light-Dark Regulation of the Chloroplast ATP Synthase. *Frontiers in Plant Science*, *8*, 1248. https://doi.org/10.3389/fpls.2017.01248

Konno, H., Nakane, T., Yoshida, M., Ueoka-Nakanishi, H., Hara, S., & Hisabori, T. (2012). Thiol Modulation of the Chloroplast ATP Synthase is Dependent on the Energization of Thylakoid Membranes. *Plant and Cell Physiology*, *53*(4), 626–634. https://doi.org/10.1093/pcp/pcs018

Kramer, D. M., & Crofts, A. R. (1989). Activation of the Chloroplast Atpase Measured by the Electrochromic Change in Leaves of Intact Plants. *Biochimica et Biophysica Acta*, *976*(1), 28–41. https://doi.org/10.1016/S0005-2728(89)80186-0

Kramer, D. M., Wise, R. R., Frederick, J. R., Alm, D. M., Hesketh, J. D., Ort, D. R., & Crofts, A. R. (1990). Regulation of Coupling Factor in Field-Grown Sunflower - a Redox Model Relating Coupling Factor Activity to the Activities of Other Thioredoxin-Dependent Chloroplast Enzymes. *Photosynthesis Research*, *26*(3), 213–222. https://doi.org/10.1007/BF00033134

Krishnan-Schmieden, M., Konold, P. E., Kennis, J. T. M., & Pandit, A. (2021). The molecular pH-response mechanism of the plant light-stress sensor PsbS. *Nature Communications*, *12*(1), 2291. https://doi.org/10.1038/s41467-021-22530-4

Lepistö, A., Kangasjärvi, S., Luomala, E.-M., Brader, G., Sipari, N., Keränen, M., Keinänen, M., & Rintamäki, E. (2009). Chloroplast NADPH-Thioredoxin Reductase Interacts with Photoperiodic Development in Arabidopsis. *Plant Physiology*, *149*(3), 1261–1276. https://doi.org/10.1104/pp.108.133777

Lima-Melo, Y., Gollan, P. J., Tikkanen, M., Silveira, J. A. G., & Aro, E.-M. (2018). Consequences of photosystem-I damage and repair on photosynthesis and carbon use in Arabidopsis thaliana. *The Plant Journal*, *0*(0). https://doi.org/10.1111/tpj.14177

Lindahl, M., & Florencio, F. J. (2003). Thioredoxin-linked processes in cyanobacteria are as numerous as in chloroplasts, but targets are different. *Proceedings of the National Academy of Sciences*, *100*(26), 16107–16112. https://doi.org/10.1073/pnas.2534397100

Llobell, A., Fernandez, V. M., & Lopezbarea, J. (1986). Electron-Transfer between Reduced Methyl Viologen and Oxidized Glutathione - a New Assay of Saccharomyces-Cerevisiae Glutathione-Reductase. *Archives of Biochemistry and Biophysics*, *250*(2), 373–381. https://doi.org/10.1016/0003-9861(86)90739-3

Maekawa, S., Ohnishi, M., Wada, S., Ifuku, K., & Miyake, C. (2024). Enhanced Reduction of Ferredoxin in PGR5-Deficient Mutant of Arabidopsis thaliana Stimulated Ferredoxin-Dependent Cyclic Electron Flow around Photosystem I. *International Journal of Molecular Sciences*, *25*(5), 2677. https://doi.org/10.3390/ijms25052677

Margulis, K., Zer, H., Lis, H., Schoffman, H., Murik, O., Shimakawa, G., Krieger-Liszkay, A., & Keren, N. (2020). Over Expression of the Cyanobacterial Pgr5-Homologue Leads to Pseudoreversion in a Gene Coding for a Putative Esterase in Synechocystis 6803. *Life*, *10*(9), 174. https://doi.org/10.3390/life10090174

Mathiot, C., & Alric, J. (2021). Standard units for ElectroChromic Shift measurements in plant biology. *Journal of Experimental Botany*, *72*(18), 6467–6473. https://doi.org/10.1093/jxb/erab261

McCarty, R. E., & Fagan, J. (1973). Light-stimulated incorporation of N-ethylmaleimide into coupling factor 1 in spinach chloroplasts. *Biochemistry*, *12*(8), 1503–1507. https://doi.org/10.1021/bi00732a006

McKinney, D. W., Buchanan, B. B., & Wolosiuk, R. A. (1978). Activation of Chloroplast Atpase by Reduced Thioredoxin. *Phytochemistry*, *17*(4), 794–795. https://doi.org/10.1016/S0031-9422(00)94230-4

Miller, N. T., Vaughn, M. D., & Burnap, R. L. (2021). Electron flow through NDH-1 complexes is the major driver of cyclic electron flow-dependent proton pumping in cyanobacteria. *Biochimica et Biophysica Acta (BBA) - Bioenergetics*, *1862*(3), 148354. https://doi.org/https://doi.org/10.1016/j.bbabio.2020.148354

Mirdita, M., Schütze, K., Moriwaki, Y., Heo, L., Ovchinnikov, S., & Steinegger, M. (2022). ColabFold: making protein folding accessible to all. *Nature Methods*, *19*(6), 679–682. https://doi.org/10.1038/s41592-022-01488-1

Munekage, Y., Hojo, M., Meurer, J., Endo, T., Tasaka, M., & Shikanai, T. (2002). PGR5 is involved in cyclic electron flow around photosystem I and is essential for photoprotection in Arabidopsis. *Cell*, *110*(3), 361–371. https://doi.org/10.1016/S0092-8674(02)00867-X

Murakami, S., Kondo, K., Katayama, S., Hara, S., Sunamura, E., Yamashita, E., Groth, G., & Hisabori, T. (2018). Structure of the γ–ε complex of cyanobacterial F1-ATPase reveals a suppression mechanism of the γ subunit on ATP hydrolysis in phototrophs. *Biochemical Journal*, *475*(18), 2925–2939. https://doi.org/10.1042/BCJ20180481

Mustila, H., Paananen, P., Battchikova, N., Santana-Sanchez, A., Muth-Pawlak, D., Hagemann, M., Aro, E.-M., & Allahverdiyeva, Y. (2016). The Flavodiiron Protein Flv3 Functions as a Homo-Oligomer During Stress Acclimation and is Distinct from the Flv1/Flv3 Hetero-Oligomer Specific to the O-2 Photoreduction Pathway. *Plant and Cell Physiology*, *57*(7), 1468–1483. https://doi.org/10.1093/pcp/pcw047

Nalin, C. M., & McCarty, R. E. (1984). Role of a Disulfide Bond in the Gamma-Subunit in Activation of the Atpase of Chloroplast Coupling Factor-i. *Journal of Biological Chemistry*, *259*(11), 7275–7280.

Nandha, B., Finazzi, G., Joliot, P., Hald, S., & Johnson, G. N. (2007). The role of PGR5 in the redox poising of photosynthetic electron transport. In *Biochimica et Biophysica Acta (BBA) - Bioenergetics* (Vol. 1767, Issue 10, pp. 1252–1259). https://doi.org///doi.org/10.1016/j.bbabio.2007.07.007

Naranjo, B., Penzler, J.-F., Rühle, T., & Leister, D. (2021). NTRC Effects on Non-Photochemical Quenching Depends on PGR5. *Antioxidants*, *10*(6), 900. https://doi.org/10.3390/antiox10060900

Nikkanen, L., Guinea Diaz, M., Toivola, J., Tiwari, A., & Rintamäki, E. (2019). Multilevel regulation of non-photochemical quenching and state transitions by chloroplast NADPH-dependent thioredoxin reductase. *Physiologia Plantarum*, *166*(1). https://doi.org/10.1111/ppl.12914

Nikkanen, L., Santana Sánchez, A., Ermakova, M., Rögner, M., Cournac, L., & Allahverdiyeva, Y. (2020). Functional redundancy between flavodiiron proteins and NDH-1 in Synechocystis sp. PCC 6803. *The Plant Journal : For Cell and Molecular Biology*, *103*(4), 1460–1476. https://doi.org/10.1111/tpj.14812 [doi]

Nikkanen, L., Solymosi, D., Jokel, M., & Allahverdiyeva, Y. (2021). Regulatory electron transport pathways of photosynthesis in cyanobacteria and microalgae: Recent advances and biotechnological prospects. *Physiologia Plantarum*, *173*, 514–525. https://doi.org/10.1111/ppl.13404

Nikkanen, L., Toivola, J., & Rintamäki, E. (2016). Crosstalk between chloroplast thioredoxin systems in regulation of photosynthesis. *Plant Cell and Environment*, *39*(8), 1691–1705. https://doi.org/10.1111/pce.12718

Nikkanen, L., Toivola, J., Trotta, A., Guinea Diaz, M., Tikkanen, M., Aro, E.-M., & Rintamäki, E. (2018). Regulation of cyclic electron flow by chloroplast NADPH-dependent thioredoxin system. *Plant Direct*, *2*(11), 1–24. https://doi.org/10.1002/pld3.93

Nikkanen, L., Vakal, S., Santana-Sánchez, A., Hubacek, M., Wang, Y., Böhm, M., Gutekunst, K., Salminen, T. A., & Allahverdiyeva, Y. (2023). Proton motive force dissipation drives flavodiiron proteins to the thylakoid membrane for ferredoxin-powered O₂ photoreduction. *BioRxiv*, 2023.05.19.541409. https://doi.org/10.1101/2023.05.19.541409

Nishikawa, Y., Yamamoto, H., Okegawa, Y., Wada, S., Sato, N., Taira, Y., Sugimoto, K., Makino, A., & Shikanai, T. (2012). PGR5-Dependent Cyclic Electron Transport Around PSI Contributes to the

Redox Homeostasis in Chloroplasts Rather Than CO2 Fixation and Biomass Production in Rice. *Plant and Cell Physiology*, *53*(12), 2117–2126. https://doi.org/10.1093/pcp/pcs153

Niyogi, K. K., & Truong, T. B. (2013). Evolution of flexible non-photochemical quenching mechanisms that regulate light harvesting in oxygenic photosynthesis. In *Current Opinion in Plant Biology* (Vol. 16, Issue 3, pp. 307–314). https://doi.org///doi.org/10.1016/j.pbi.2013.03.011

Okegawa, Y., & Motohashi, K. (2020). M-type thioredoxins regulate the PGR5/PGRL1-dependent pathway by forming a disulfide-linked complex with PGRL1. *Plant Cell*, *32*(12), 3866–3883. https://doi.org/10.1105/tpc.20.00304

Ortega-Martínez, P., Nikkanen, L., Wey, L. T., Florencio, F. J., Allahverdiyeva, Y., & Díaz-Troya, S. (2024). Glycogen synthesis prevents metabolic imbalance and disruption of photosynthetic electron transport from photosystem <scp>II</scp> during transition to photomixotrophy in *Synechocystis* sp. <scp>PCC</scp> 6803. *New Phytologist*, *243*(1), 162–179. https://doi.org/10.1111/nph.19793

Penzler, J.-F., Marino, G., Reiter, B., Kleine, T., Naranjo, B., & Leister, D. (2022). Commonalities and specialties in photosynthetic functions of PROTON GRADIENT REGULATION5 variants in Arabidopsis. *Plant Physiology*, *190*(3), 1866–1882. https://doi.org/10.1093/plphys/kiac362

Pérez-Ruiz, J. M., Naranjo, B., Ojeda, V., Guinea, M., & Cejudo, F. J. (2017). NTRC-dependent redox balance of 2-Cys peroxiredoxins is needed for optimal function of the photosynthetic apparatus. *Proceedings of the National Academy of Sciences*, *114*(45), 12069–12074. https://doi.org/10.1073/pnas.1706003114

Puerto-Galan, L., Perez-Ruiz, J. M., Ferrandez, J., Cano, B., Naranjo, B., Najera, V. A., Gonzalez, M., Lindahl, A. M., & Cejudo, F. J. (2013). Overoxidation of chloroplast 2-Cys peroxiredoxins: balancing toxic and signaling activities of hydrogen peroxide. *Frontiers in Plant Science*, *4*, 310. https://doi.org/10.3389/fpls.2013.00310

Rantala, S., Lempiäinen, T., Gerotto, C., Tiwari, A., Aro, E. M., & Tikkanen, M. (2020). PGR5 and NDH-1 systems do not function as protective electron acceptors but mitigate the consequences of PSI inhibition. *Biochimica et Biophysica Acta - Bioenergetics*, *1861*(3). https://doi.org/10.1016/j.bbabio.2020.148154

Rey, P., Henri, P., Alric, J., Blanchard, L., & Viola, S. (2024). Participation of the stress-responsive CDSP32 thioredoxin in the modulation of chloroplast ATP-synthase activity in *Solanum tuberosum*. *Plant, Cell & Environment*. https://doi.org/10.1111/pce.15101

Richter, M. L., & McCarty, R. E. (1987). Energy-dependent changes in the conformation of the epsilon subunit of the chloroplast ATP synthase. *Journal of Biological Chemistry*, *262*(31), 15037–15040. https://doi.org/10.1016/S0021-9258(18)48134-3

Rühle, T., Dann, M., Reiter, B., Schünemann, D., Naranjo, B., Penzler, J.-F., Kleine, T., & Leister, D. (2021). PGRL2 triggers degradation of PGR5 in the absence of PGRL1. *Nature Communications*, *12*(1), 3941. https://doi.org/10.1038/s41467-021-24107-7

Sacksteder, C. A., & Kramer, D. M. (2000). Dark-interval relaxation kinetics (DIRK) of absorbance changes as a quantitative probe of steady-state electron transfer. *Photosynthesis Research*, *66*(1–2), 145–158. https://doi.org/1010785912271

Santana-Sánchez, A., Nikkanen, L., Werner, E., Tóth, G., Ermakova, M., Kosourov, S., Walter, J., He, M., Aro, E., & Allahverdiyeva, Y. (2023). Flv3A facilitates O2 photoreduction and affects H2 photoproduction independently of Flv1A in diazotrophic Anabaena filaments. *New Phytologist*, *237*(1), 126–139. https://doi.org/10.1111/nph.18506

Santana-Sanchez, A., Solymosi, D., Mustila, H., Bersanini, L., Aro, E.-M., & Allahverdiyeva, Y. (2019). Flavodiiron proteins 1-to-4 function in versatile combinations in O-2 photoreduction in cyanobacteria. *Elife*, *8*, e45766. https://doi.org/10.7554/eLife.45766

Schreiber, U., & Klughammer, C. (2008). New accessory for the DUAL-PAM-100: The P515/535 module and examples of its application. *PAM Application Notes*, *1*, 1–10.

Schreiber, U., Klughammer, C., & Walz, H. (2008). *Complementary PS II quantum yields calculated from simple fluorescence parameters measured by PAM fluorometry and the Saturation Pulse method* (Vol. 1). http://www.walz.com/http://www.walz.com/

Schwarz, O., Schürmann, P., & Strotmann, H. (1997). Kinetics and thioredoxin specificity of thiol modulation of the chloroplast H+-ATPase. *Journal of Biological Chemistry*, *272*(27), 16924–16927. https://doi.org/10.1074/jbc.272.27.16924

Sehnal, D., Bittrich, S., Deshpande, M., Svobodová, R., Berka, K., Bazgier, V., Velankar, S., Burley, S. K., Koča, J., & Rose, A. S. (2021). Mol* Viewer: modern web app for 3D visualization and analysis of large biomolecular structures. *Nucleic Acids Research*, *49*(W1), W431–W437. https://doi.org/10.1093/nar/gkab314

Sekiguchi, T., Yoshida, K., Okegawa, Y., Motohashi, K., Wakabayashi, K., & Hisabori, T. (2020). Chloroplast ATP synthase is reduced by both f-type and m-type thioredoxins. *Biochimica et Biophysica Acta (BBA) - Bioenergetics*, *1861*(11), 148261. https://doi.org/10.1016/j.bbabio.2020.148261

Sekiguchi, T., Yoshida, K., Wakabayashi, K., & Hisabori, T. (2024). Proton gradient across the chloroplast thylakoid membrane governs the redox regulatory function of ATP synthase. *Journal of Biological Chemistry*, *300*(9), 107659. https://doi.org/10.1016/j.jbc.2024.107659

Sekiguchi, T., Yoshida, K., Wakabayashi, K.-I., & Hisabori, T. (2022). Dissipation of the proton electrochemical gradient in chloroplasts promotes the oxidation of ATP synthase by thioredoxin-like proteins. *Journal of Biological Chemistry*, *298*(11), 102541. https://doi.org/10.1016/j.jbc.2022.102541

Sétif, P. (2015). Electron-transfer kinetics in cyanobacterial cells: Methyl viologen is a poor inhibitor of linear electron flow. *Biochimica et Biophysica Acta (BBA) - Bioenergetics*, *1847*(2), 212–222. https://doi.org/10.1016/j.bbabio.2014.10.008

Shapiguzov, A., Nikkanen, L., Fitzpatrick, D., Vainonen, J. P., Gossens, R., Alseekh, S., Aarabi, F., Tiwari, A., Blokhina, O., Panzarová, K., Benedikty, Z., Tyystjärvi, E., Fernie, A. R., Trtílek, M., Aro,

E.-M., Rintamäki, E., & Kangasjärvi, J. (2020). Dissecting the interaction of photosynthetic electron transfer with mitochondrial signalling and hypoxic response in the Arabidopsis rcd1 mutant. *Philosophical Transactions of the Royal Society B: Biological Sciences*, *375*(1801). https://doi.org/10.1098/rstb.2019.0413

Shapiguzov, A., Vainonen, J. P., Hunter, K., Tossavainen, H., Tiwari, A., Järvi, S., Hellman, M., Aarabi, F., Alseekh, S., Wybouw, B., van der Kelen, K., Nikkanen, L., Krasensky-Wrzaczek, J., Sipari, N., Keinänen, M., Tyystjärvi, E., Rintamäki, E., De Rybel, B., Salojärvi, J., … Kangasjärvi, J. (2019). Arabidopsis RCD1 coordinates chloroplast and mitochondrial functions through interaction with ANAC transcription factors. *ELife*, *8*. https://doi.org/10.7554/eLife.43284

Shimakawa, G., Shaku, K., & Miyake, C. (2016). Oxidation of P700 in Photosystem I Is Essential for the Growth of Cyanobacteria. *Plant Physiology*, *172*(3), 1443–1450. https://doi.org/10.1104/pp.16.01227

Solymosi, D., Nikkanen, L., Muth-Pawlak, D., Fitzpatrick, D., Vasudevan, R., Howe, C. J., Lea-Smith, D. J., & Allahverdiyeva, Y. (2020). Cytochrome cM decreases photosynthesis under photomixotrophy in synechocystis sp. PCC 6803. *Plant Physiology*, *183*(2). https://doi.org/10.1104/pp.20.00284

Song, K., Baumgartner, D., Hagemann, M., Muro-Pastor, A. M., Maaß, S., Becher, D., & Hess, W. R. (2022). AtpΘ is an inhibitor of F0F1 ATP synthase to arrest ATP hydrolysis during low-energy conditions in cyanobacteria. *Current Biology*, *32*(1), 136-148.e5. https://doi.org/10.1016/j.cub.2021.10.051

Soteropoulos, P., Ong, A. M., & McCarty, R. E. (1994). Alkylation of cysteine 89 of the gamma subunit of chloroplast coupling factor 1 with N-ethylmaleimide alters nucleotide interactions. *Journal of Biological Chemistry*, *269*(31), 19810–19816. https://doi.org/10.1016/S0021-9258(17)32092-6

Spetea, C., Herdean, A., Allorent, G., Carraretto, L., Finazzi, G., & Szabo, I. (2017). An update on the regulation of photosynthesis by thylakoid ion channels and transporters in Arabidopsis. *Physiologia Plantarum*, *161*(1), 16–27. https://doi.org/10.1111/ppl.12568

Sunamura, E.-I., Konno, H., Imashimizu-Kobayashi, M., Sugano, Y., & Hisabori, T. (2010). Physiological Impact of Intrinsic ADP Inhibition of Cyanobacterial FoF1 Conferred by the Inherent Sequence Inserted into the γ Subunit. *Plant and Cell Physiology*, *51*(6), 855–865. https://doi.org/10.1093/pcp/pcq061

Suorsa, M., Jarvi, S., Grieco, M., Nurmi, M., Pietrzykowska, M., Rantala, M., Kangasjarvi, S., Paakkarinen, V., Tikkanen, M., Jansson, S., & Aro, E.-M. (2012). PROTON GRADIENT REGULATION5 Is Essential for Proper Acclimation of Arabidopsis Photosystem I to Naturally and Artificially Fluctuating Light Conditions. *Plant Cell*, *24*(7), 2934–2948. https://doi.org/10.1105/tpc.112.097162

Takagi, D., Amako, K., Hashiguchi, M., Fukaki, H., Ishizaki, K., Goh, T., Fukao, Y., Sano, R., Kurata, T., Demura, T., Sawa, S., & Miyake, C. (2017). Chloroplastic ATP synthase builds up a proton motive force preventing production of reactive oxygen species in photosystem I. *Plant Journal*, *91*(2), 306–324. https://doi.org/10.1111/tpj.13566

Takagi, D., & Miyake, C. (2018). PROTON GRADIENT REGULATION 5 supports linear electron flow to oxidize photosystem I. *Physiologia Plantarum*, *164*(3), 337–348. https://doi.org/10.1111/ppl.12723

Theune, M. L., Hildebrandt, S., Steffen-Heins, A., Bilger, W., Gutekunst, K., & Appel, J. (2021). In-vivo quantification of electron flow through photosystem I – Cyclic electron transport makes up about 35% in a cyanobacterium. *Biochimica et Biophysica Acta (BBA) - Bioenergetics*, *1862*(3), 148353. https://doi.org/10.1016/j.bbabio.2020.148353

Tikhonov, A. N., Khomutov, G. B., Ruuge, E. K., & Blumenfeld, L. A. (1981). Electron transport control in chloroplasts. Effects of photosynthetic control monitored by the intrathylakoid pH. *Biochimica et Biophysica Acta (BBA) - Bioenergetics*, *637*(2), 321–333. https://doi.org/10.1016/0005-2728(81)90171-7

Tikkanen, M., & Aro, E. M. (2014). Integrative regulatory network of plant thylakoid energy transduction. *Trends in Plant Science*, *19*(1), 10–17. https://doi.org/10.1016/j.tplants.2013.09.003 [doi]

Tikkanen, M., Grieco, M., Kangasjarvi, S., & Aro, E.-M. (2010). Thylakoid Protein Phosphorylation in Higher Plant Chloroplasts Optimizes Electron Transfer under Fluctuating Light. *Plant Physiology*, *152*(2), 723–735. https://doi.org/10.1104/pp.109.150250

Tikkanen, M., Rantala, S., & Aro, E.-M. (2015). Electron flow from PSII to PSI under high light is controlled by PGR5 but not by PSBS. *Frontiers in Plant Science*, *6*, 521. https://doi.org/10.3389/fpls.2015.00521

Tiwari, A., Mamedov, F., Fitzpatrick, D., Gunell, S., Tikkanen, M., & Aro, E.-M. (2024). Differential FeS cluster photodamage plays a critical role in regulating excess electron flow through photosystem I. *Nature Plants*. https://doi.org/10.1038/s41477-024-01780-2

Tiwari, A., Mamedov, F., Grieco, M., Suorsa, M., Jajoo, A., Styring, S., Tikkanen, M., & Aro, E.-M. (2016). Photodamage of iron-sulphur clusters in photosystem I induces non-photochemical energy dissipation. *Nature Plants*, *2*(4), 16035. https://doi.org/10.1038/NPLANTS.2016.35

Vaseghi, M.-J., Chibani, K., Telman, W., Liebthal, M. F., Gerken, M., Schnitzer, H., Mueller, S. M., & Dietz, K.-J. (2018). The chloroplast 2-cysteine peroxiredoxin functions as thioredoxin oxidase in redox regulation of chloroplast metabolism. *ELife*, *7*, e38194. https://doi.org/10.7554/eLife.38194

Vialet-Chabrand, S., Matthews, J. S. A., Simkin, A. J., Raines, C. A., & Lawson, T. (2017). Importance of Fluctuations in Light on Plant Photosynthetic Acclimation. *Plant Physiology*, *173*(4), 2163–2179. https://doi.org/10.1104/pp.16.01767

Viola, S., Bailleul, B., Yu, J., Nixon, P., Selles, J., Joliot, P., & Wollman, F.-A. (2019). Probing the electric field across thylakoid membranes in cyanobacteria. *Proceedings of the National Academy of Sciences of the United States of America*, *116*(43), 21900–21906. https://doi.org/10.1073/pnas.1913099116

von Bismarck, T., Korkmaz, K., Ruß, J., Skurk, K., Kaiser, E., Correa Galvis, V., Cruz, J. A., Strand, D. D., Köhl, K., Eirich, J., Finkemeier, I., Jahns, P., Kramer, D. M., & Armbruster, U. (2023). Light acclimation interacts with thylakoid ion transport to govern the dynamics of photosynthesis in Arabidopsis. *New Phytologist*, *237*(1), 160–176. https://doi.org/10.1111/nph.18534

Wada, S., Amako, K., & Miyake, C. (2021). Identification of a Novel Mutation Exacerbated the PSI Photoinhibition in pgr5/pgrl1 Mutants; Caution for Overestimation of the Phenotypes in Arabidopsis pgr5-1 Mutant. *Cells*, *10*(11), 2884. https://doi.org/10.3390/cells10112884

Wang, C., & Shikanai, T. (2019). Modification of Activity of the Thylakoid H+/K+ Antiporter KEA3 Disturbs Delta pH-Dependent Regulation of Photosynthesis. *Plant Physiology*, *181*(2), 762–773. https://doi.org/10.1104/pp.19.00766

Wang, C., Takahashi, H., & Shikanai, T. (2018). PROTON GRADIENT REGULATION 5 contributes to ferredoxin-dependent cyclic phosphorylation in ruptured chloroplasts. *Biochimica Et Biophysica Acta-Bioenergetics*, *1859*(10), 1173–1179. https://doi.org/10.1016/j.bbabio.2018.07.011

Wang, C., Yamamoto, H., & Shikanai, T. (2015). Role of cyclic electron transport around photosystem I in regulating proton motive force. *Biochimica Et Biophysica Acta-Bioenergetics*, *1847*(9), 931–938. https://doi.org/10.1016/j.bbabio.2014.11.013

Wolf, B., Isaacson, T., Tiwari, V., Dangoor, I., Mufkadi, S., & Danon, A. (2020). Redox regulation of PGRL1 at the onset of low light intensity. *The Plant Journal*, *103*(2), 715–725. https://doi.org/10.1111/tpj.14764

Woodford, R., Watkins, J., Moore, M., Nix, S. J., Yee, S., Chan, K. X., Pogson, B. J., von Caemmerer, S., Furbank, R. T., & Ermakova, M. (2024). PGR5 promotes energy-dependent non-photochemical quenching to enable efficient C4 photosynthesis under fluctuating light. *BioRxiv*, 2024.09.15.613160. https://doi.org/10.1101/2024.09.15.613160

Wu, X., Wu, J., Wang, Y., He, M., He, M., Liu, W., Shu, S., Sun, J., & Guo, S. (2021). The key cyclic electron flow protein PGR5 associates with cytochrome b6f, and its function is partially influenced by the LHCII state transition. *Horticulture Research*, *8*(1), 55. https://doi.org/10.1038/s41438-021-00460-y

Yamamoto, H., & Shikanai, T. (2019). PGR5-Dependent Cyclic Electron Flow Protects Photosystem I under Fluctuating Light at Donor and Acceptor Sides. *Plant Physiology*, pp.01343.2018. https://doi.org/10.1104/pp.18.01343

Yamamoto, H., & Shikanai, T. (2020). Does the Arabidopsis *proton gradient regulation5* Mutant Leak Protons from the Thylakoid Membrane? *Plant Physiology*, *184*(1), 421–427. https://doi.org/10.1104/pp.20.00850

Yeremenko, N., Jeanjean, R., Prommeenate, P., Krasikov, V., Nixon, P. J., Vermaas, W. F. J., Havaux, M., & Matthijs, H. C. P. (2005). Open reading frame ssr2016 is required for antimycin A-sensitive photosystem I-driven cyclic electron flow in the cyanobacterium Synechocystis sp PCC 6803. *Plant and Cell Physiology*, *46*(8), 1433–1436. https://doi.org/10.1093/pcp/pci147

Zhang, P., Allahverdiyeva, Y., Eisenhut, M., & Aro, E.-M. (2009). Flavodiiron Proteins in Oxygenic Photosynthetic Organisms: Photoprotection of Photosystem II by Flv2 and Flv4 in Synechocystis sp PCC 6803. *Plos One*, *4*(4), e5331. https://doi.org/10.1371/journal.pone.0005331

Zhou, Q., Yamamoto, H., & Shikanai, T. (2023). Distinct contribution of two cyclic electron transport pathways to P700 oxidation. *Plant Physiology*, *192*(1), 326–341. https://doi.org/10.1093/plphys/kiac557

Zimmer, D., Swart, C., Graf, A., Arrivault, S., Tillich, M., Proost, S., Nikoloski, Z., Stitt, M., Bock, R., Mühlhaus, T., & Boulouis, A. (2021). Topology of the redox network during induction of photosynthesis as revealed by time-resolved proteomics in tobacco. *Science Advances*, *7*(51). https://doi.org/10.1126/sciadv.abi8307